Chapter 3

Field experiments investigating the self-heating behaviour of large scale stockpiles of low symmetry

3.1. Introduction.

The model described by Macaskill, Sexton and Gray (1998) uses the exothermic oxidation reactions of bagasse as well as condensation, evaporation and moisture diffusion processes to calculate the self-heating behaviour of bagasse stockpiles.

A study of the literature revealed a paucity of detailed experimental studies regarding the behaviour of bagasse stockpiles against which model predictions could be tested. This chapter describes data obtained from bagasse stockpiles of 'one dimensional' geometry that were constructed and instrumented with the objective of testing the theoretical model developed by Macaskill et al.

3.2. Design Criteria and General Objectives.

Model calculations were completed to determine the optimal widths of the first experimental stockpiles. These calculations utilised the very limited amount of heat release data obtained from the initial laboratory measurements discussed in chapter 2 as well as an early version of the Macaskill et al. (1998) model, which could predict the self-heating behaviour of simple 1-dimensional stockpiles only. The preferred geometry was determined to be a vertically standing infinite slab since the boundary condition symmetry of this very simple geometry simplified the theoretical calculations of the Macaskill et al. (1998) model. This vertical geometry also eliminated the problems associated with moisture ingress from rain, which would need to be accounted for with a horizontal slab. The calculations suggested that two separate infinite slabs of bagasse with thickness of 1.2m and 0.5m would each self-heat to similar centre temperatures. To investigate the accuracy of this prediction, the author designed and erected two, freestanding vertical slabs of bagasse at the Sugar Research Institute (Mackay, Queensland) over the period from August to early December 1997. The objective was to provide experimental evidence with which the predictions of the reaction diffusion model of bagasse could be compared. After due consideration of the logistical and economic aspects of this experiment,

it was decided to construct the first two stockpiles with dimensions 1.2m x 8m x 8m and 0.5m x 5m x 5m. During October and November of the following year, the experimental study was extended to investigate the density dependence of the self-heating chemistry. The latter study utilised high-density bales of bagasse assembled to form a stockpile with geometry that approximated that of an infinite slab. The results of the density study are also discussed in this chapter and compared to the predictions of the reaction diffusion model.

Figure 3.2.1 shows a view of the largest stockpile erected in this study.

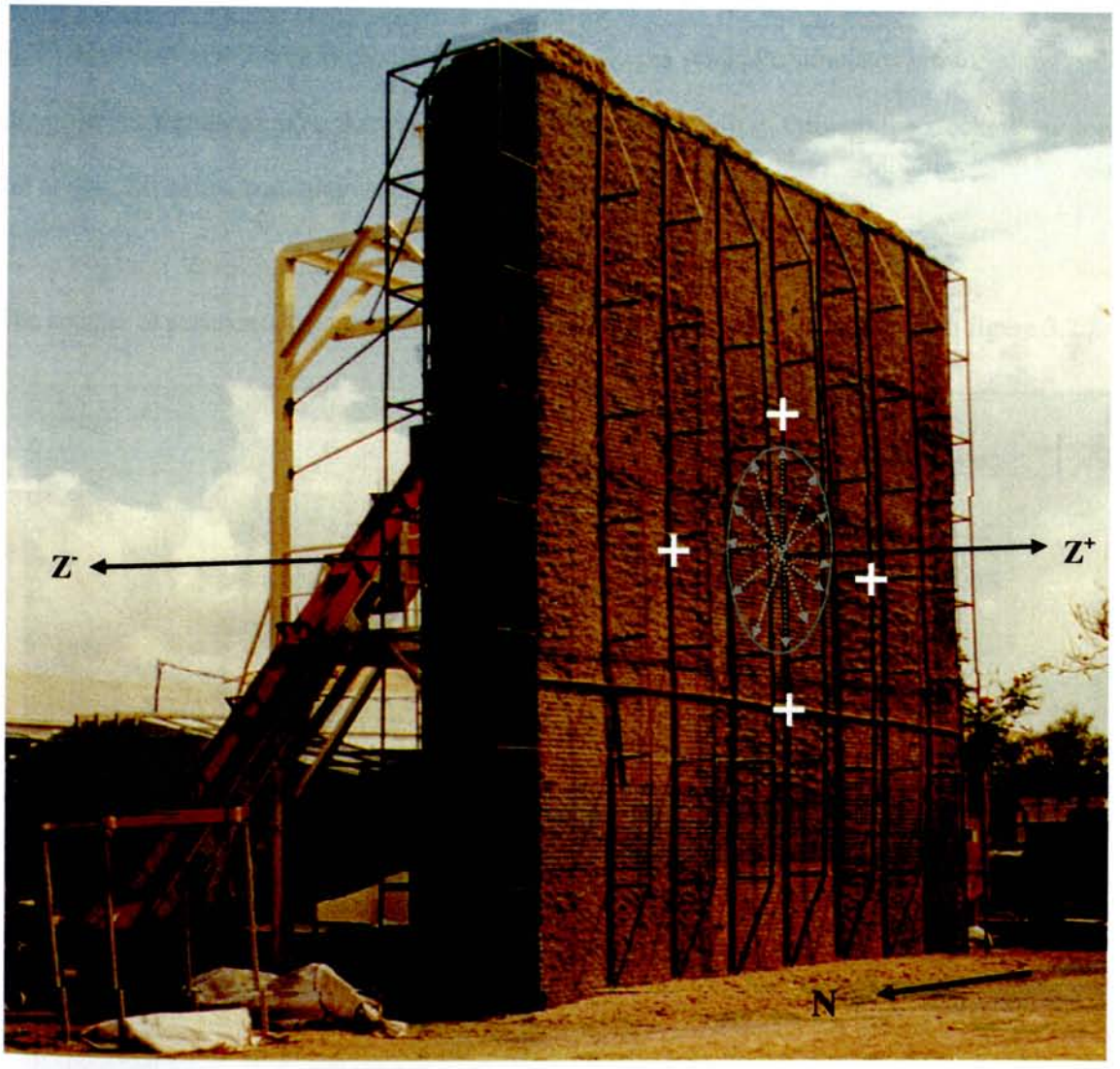

Figure 3.2.1: The completed 1.2m stockpile.

As can be seen from figure 3.2.1, the stockpile was essentially a large, wire mesh covered, narrow prism of bagasse. The main axis under investigation is identified in the above figure by the axis vectors Z^+ and Z^-, along which were installed thirteen thermojunctions and seven gas-sampling lines at equally spaced intervals. Throughout this study, the Z^+/ Z^- axis will be identified as the instrumented axis. The grey vectors radiating from this axis will be identified as the radial axes and indicate the 'infinitely' large plane that is aligned orthogonal to the instrumented axis. The four narrow surfaces that bound the perimeter of the stockpile in the radial directions will be identified as the radial surfaces, while the surfaces that bound each side of the instrumented axis, will be identified as either the easterly or the westerly surface. To investigate the magnitude of the thermal gradients along the radial directions and therefore evaluate how effectively the stockpile simulates infinite slab conditions along the instrumented axis, thermojunctions were located midway through the stockpile at positions 2m above, 2m below and 2m to each side of the instrumented axis.

The smaller experimental stockpile with dimensions of 5m x 5m x 0.5m, is shown in figure 3.2.2.

Figure 3.2.2: The 0.5m and 1.2m stockpiles from a southeasterly aspect. The 0.5m stockpile was photographed just following filling operation. The excess bagasse, at the side of the 0.5m stockpile was later removed.

In the above figure, the instrumented axis and the positions of the radial thermojunctions are shown in a similar manner to figure 3.2.1. In this case, six thermojunctions and five gas sampling lines were installed across the instrumented axis while the radial thermojunctions were positioned 1.25m from the instrumented axis. In this figure, the 1.2m stockpile can be seen behind the 0.5m stockpile. The rail car that was used to house the logging equipment can also be seen on the left hand side of this figure while the aerially suspended 'catenary' mains power, telephone and compressed air supply lines that extended from the rail car, are also visible.

3.3. Design of the vertical supporting structures.

The author of this thesis undertook all aspects of this study including:

- the structural design and fabrication of the steel cages (including all welding, etc),
- the design, assembly/construction and installation of all instrumentation and computer controlled logging equipment, including the compilation of the automation software,
- the physical loading of the bagasse into the cages,
- the remote downloading and data reduction of the logged data and
- the transportation of the 13 tonnes of bagasse in the form of bales from 'Invicta' Sugar refining Mill, Townsville to the Sugar Research Institute, Mackay.

Assistance was utilised only during the process of raising the steel cages into the erect position, during the actual bagasse filling operation and following computer problems that were unable to be solved remotely from Sydney.

Due to imposed funding restrictions, the supporting structures were designed to contain the bagasse with a minimum amount of structural material. To maximize structural efficiency, the final design featured fabricated steel trusses and fabricated hollow boxed frames throughout. Although this design minimised steel costs, it correspondingly maximised the welding and fabrication requirements and as such, an extensive amount of welding was required due to the use of thin gauge tubing. All steel joints were fully welded to maximise the joint load bearing area and minimise the possibility of failure.

Bagasse, being a fibrous material, does not flow easily since the fibres tend to interlock together and inhibit the horizontal movement of the bulk material. Calculations showed that horizontal loads would be exerted onto the steel mesh surface of each cage primarily during the filling operation and during high wind conditions. At other times, the bagasse would be essentially self-supporting. This attribute facilitated further cost reductions by reducing the number and size of the steel members required to support the horizontal loads. The steel bracing that was used to maintain the 1.2m cage in the vertical position, is shown in figure 3.3.1

Figure 3.3.1: A side view of the cage from a northerly aspect.

Each of the steel struts shown in figure 3.3.1 was fully welded to the pre-existing white coloured steel structure. A corresponding number of struts were used to brace the southern end of the cage.

3.4. Fabrication

Each cage was fabricated from 25mm × 25mm × 1.6mm rectangular hollow section (RHS) steel tube, 3mm thick steel angle bar and 3mm × 25mm flat bar. The cage consisted of essentially four components: the supporting tubular vertical end frames, the horizontal 'ladder like' steel frames that joined between the two vertical 'end frames,' the side trusses and the steel mesh. Figure 3.4.1 shows an exploded schematic view of the individual components of the cage.

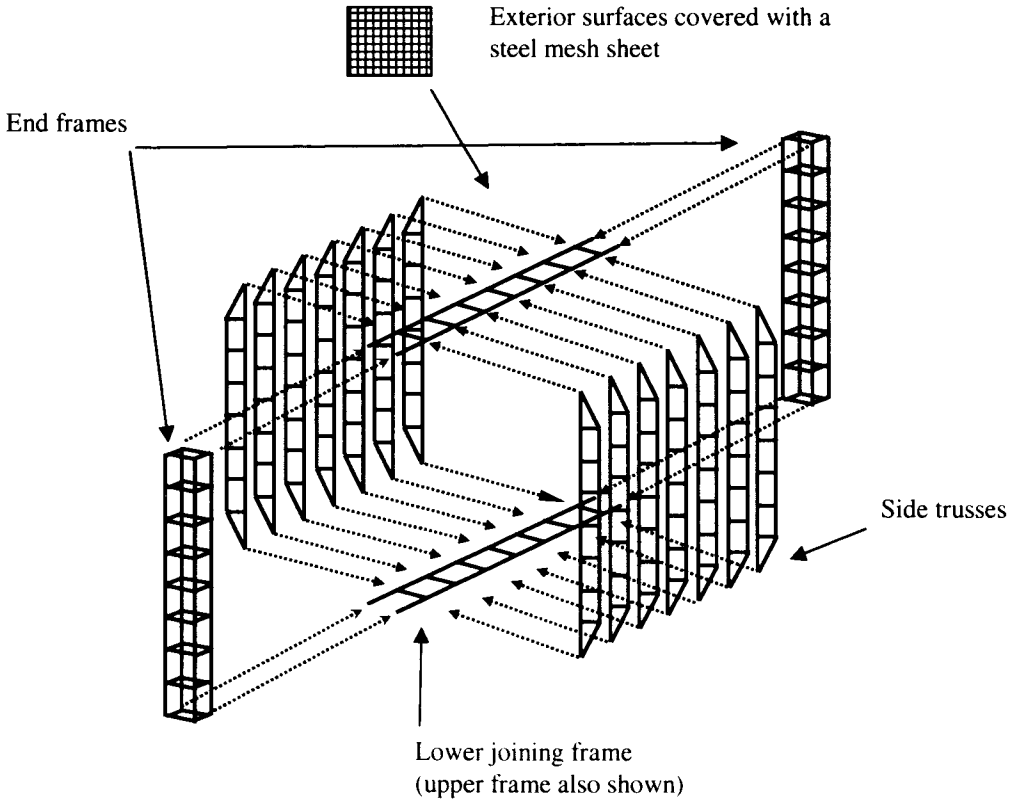

Figure 3.4.1: Exploded schematic diagram of the main components of the bagasse supporting cage.

Each of the components shown in figure 3.4.1 was separately fabricated and then the entire cage assembled in a position that would enable the completed cage to be raised directly into its final position. Once the entire steel support structure was assembled, the mesh sheets, which consisted of a

25mm x 50 mm galvanized steel wire weave with a 3mm wire diameter, were attached to the structural members as shown in figure 3.4.2.

Figure 3.4.2: The 1.2m stockpile cage under construction.

Figure 3.4.2 shows the 1.2m stockpile cage under construction in a horizontal position. Notice also the partly completed 0.5m cage towards the right hand side of this figure. The 1.2m wide cage in the foreground was raised into the vertical position using a forklift truck and hand winch. The completed 1.2m stockpile cage, ready to be filled with bagasse, is shown in figure 3.4.3

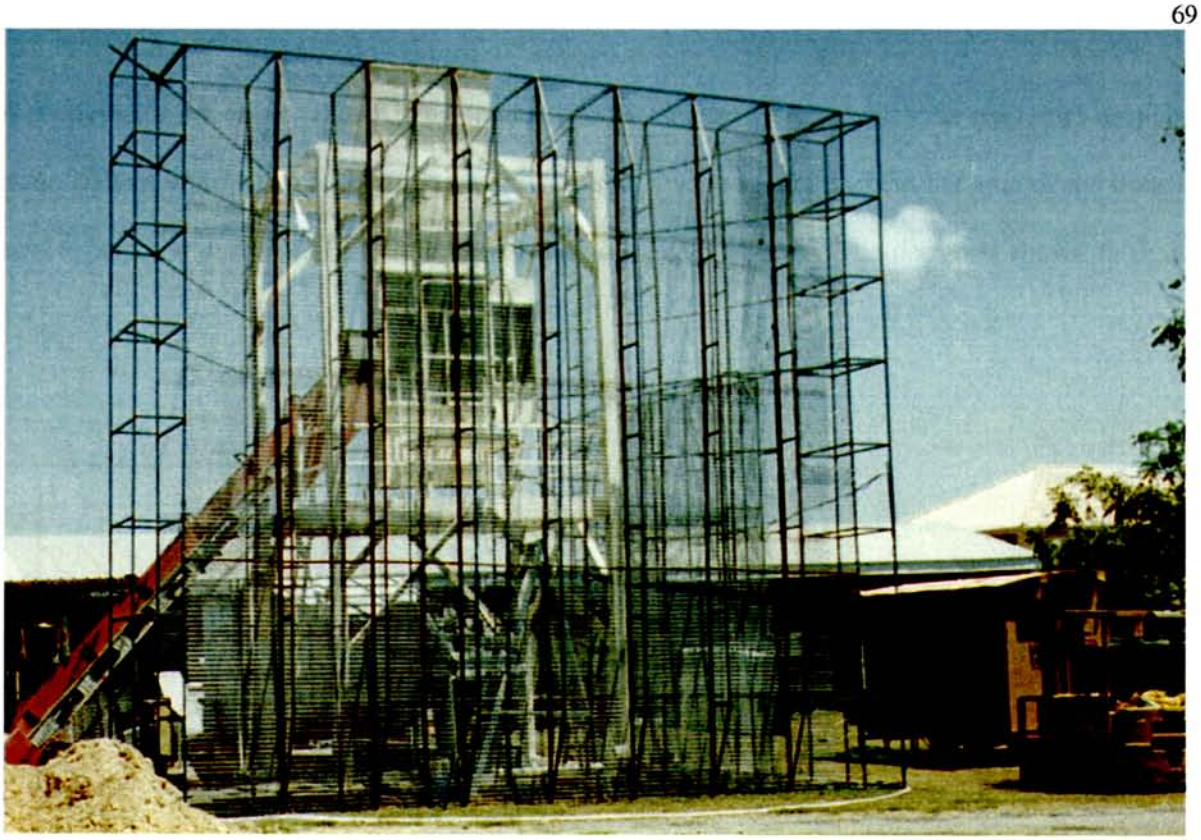

Figure 3.4.3: The 1.2m cage in the vertical position before filling

Figure 3.4.4 shows the seven 8m long vertical steel trusses welded at 1m intervals over the 8m × 8m westerly side. The open weave of the steel mesh is also shown.

Figure 3.4.4: The 1.2m stockpile when viewed from a northwesterly aspect.

A detail that is not clearly shown in the above figure is the manner with which the steel truss members made contact with the steel mesh. An unusual design was used that enabled the area of the truss in direct contact with the steel mesh to be reduced to a width of 6mm. The design is shown in figure 3.4.5.

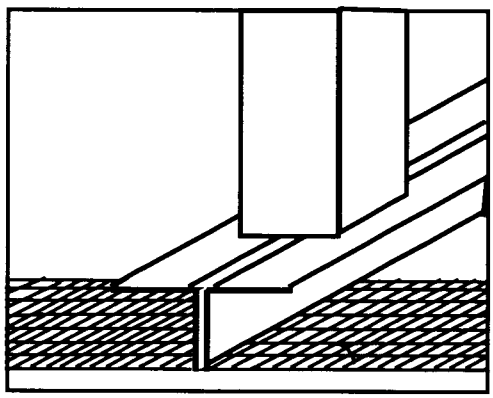

Figure 3.4.5: Schematic diagram of the contact arrangements between the truss members and the steel mesh sheet.

With the above design, the bulk of the steel work supporting the bagasse was spaced approximately 25mm away from the bagasse surface. Hence, a minimal amount of the bagasse was in contact with the steelwork and as such, the steelwork had minimal impact upon the free flow of ambient air near the surface of the bagasse.

The 0.5m stockpile was constructed and positioned in a similar manner to the larger stockpile.

3.5. Filling

The loading of the bagasse into the two supporting cages involved the use of a crane, a "back-hoe" loader and commercial 1 tonne bulk fertiliser bags. The bulk fertiliser bag was equipped with a large upper opening and four lifting loops that were sewn onto the top of the bag at equally spaced intervals around the upper opening. The filling process involved attaching the bag, by way of the four loops, to

a custom manufactured apparatus that maintained the bag in an open state. The front-end loader was then used to fill the open bag with ~0.5m^3 of bagasse as shown in figure 3.5.1.

Figure 3.5.1: The 1.2m stockpile during the filling operation.
(The author s shown dispersing the bagasse within the cage)

After loading the bag with bagasse, a separate lifting hook from the crane was attached to each of the four corner lifting loops attached to the bag and then the bag and bagasse sample raised from the steel apparatus and placed carefully into the cage. The lifting hooks were then removed, the bag rolled over, the lifting hooks attached to the underside of the bag by way of a single loop that was sewn into the base of the bag. The now inverted bag was raised and the exiting bagasse manually dispersed to form a layer of bagasse approximately 100mm thick. The bagasse was compressed by a 76kg human mass in an effort to produce relatively uniform density.

The above filling process was repeated until the stockpile was filled to a height of 2m. At this time, a thermojunction was positioned midway across the 1.2m axis and two metres directly below the position of the instrumented axis. Loading continued until a fill height of four metres was reached at which point the thermojunctions and the stainless steel gas sampling lines were installed across the

instrumented axis. Thirteen thermojunctions and five stainless steel gas sampling lines were installed. Attached to the sampling end of each of the five 3.1 mm diameter gas sampling lines was a custom manufactured 0.1mm 'mesh' stainless steel gauge filter. A further two thermojunctions were located at positions midway through the slab but at a horizontal distance of 2m to each side of the instrumented axis. The stainless steel sampling tubes and thermocouple wires were aligned perpendicular to the instrumented axis and were passed through the stockpile, along a radial dimension, for a distance of 4m before exiting the bagasse. Filling continued until a height of 6m was reached at which time a final thermocouple was located at a position midway through the slab and two metres above the instrumented axis. The stockpile was eventually filled to a level of approximately 8.5m. The 0.5m wide stockpile was filled in a similar manner to that of the 1.2m wide stockpile.

3.6. Instrumentation

Gas analysis and computer instrumentation hardware were housed within an air-conditioned railway car that was located a few metres away from the stockpiles. Mains power, compressed air supply lines and telephone services were aerially extended to the railway car from a mains supply position that was located approximately 30 metres away. Power to critical instrumentation was continuously maintained through a mains power filter and uninterrupted power supply (UPS). A single UPS, however, was found to be unreliable as the batteries aged and caused the logging computer to intermittently fail. Since funding was not made available for the purchase of a second UPS to eliminate this problem, the computer code was reprogrammed partway through this study to compensate for the unreliable nature of electrical power.

After the filling of the 1.2m stockpile, the thermocouple sensors displayed unacceptable electronic noise levels. The problem only becoming evident when the thermocouple wires were elevated several metres above the ground and was traced to radio interference from a nearby high-powered radio transmitter and vehicular based, mobile transmitters. This problem was overcome by the installation of a 'low-pass' frequency filter to each thermocouple sensor. The installation of these filters, however, resulted in delaying the commencement of automated temperature logging by two days. During this

initial period, however, a number of manual temperature measurements were recorded using the reference thermocouple meter.

All instrumentation was fully automated and could be remotely controlled and/or reprogrammed from Sydney when required.

3.7. Gas sampling and analysis

Stockpile gas samples were analysed using an automated 'GOWMAC 550' series gas chromatograph (GC) equipped with a thermal conductivity detector (TCD). A "CTR", combined molecular sieve and poraplot Q, chromatography column was installed within this GC, providing quantification of O_2, N_2, CO_2 concentrations down to approximately 1000ppm. CO could also be identified, but only above concentrations of approximately 2000ppm.

Helium (BOC UHP grade) was used as a 'carrier' gas for the above GC. To conserve helium and to reduce the need of assistance from Mackay based SRI staff, the flow control of carrier gas to the GC was automated. Through a combination of pressure sensors, regulators, automated on/off valves and automated changeover valves, the supply of helium could be automatically selected from one of two gas cylinders. The system was capable of monitoring the contents of each cylinder so that when one cylinder was exhausted, the alternate cylinder could be selected. The carrier gas was further conditioned by passing it through separate moisture (anhydrous potassium perchlorate) and oxygen (Alltech 'OXY-TRAP') scrubbing traps. The procedure for the regeneration of the GC column was also automated. The GC was regularly calibrated by directly comparing the response of the TCD to a standard calibration gas ('Scott Specialty Gases', SCOTTY® II 'MIX 218' and SCOTTY® II 'MIX 217')

Within the stockpile, the gas sample was transported through 3mm stainless steel tubing, while outside of the stockpile, 3mm high-density polyurethane tubing was used. Close to the position where the sample tubing exited the stockpile, a custom manufactured water "catchpot" was installed into the

sample line collect condensate from the gas sample. The tubing prior to the catchpot was aligned with a continuous downward gradient to facilitate liquid collection within the water trap. The sample gas stream was then passed through an automated stream selective valve, a diaphragm pump and a custom manufactured TCD flow meter, before entering the injection loop of the GC. A modified TCD flow meter was used to ensure adequate sample flow to the GC and was monitored by the logging computer. The total dead space volume within the sampling system was approximately $12cm^3$.

Gas samples were collected at approximately bi-weekly intervals. This cycle time was chosen to minimize the influence of the gas sampling operation upon the local gas concentration at the stockpile sampling positions. It was also expected that the changes in gas concentration within the stockpile would be sufficiently slow that more regular sampling would not be required. The sampling operation could be run in a fully automated mode or remotely from Sydney. Throughout this study, the remote operation and calibration of the GC proved to be a most challenging task.

The thermocouples used to measure the bagasse temperature within each stockpile were of a 'tight tolerance' (type 'TT', ± 0.5°C) copper constantan type. After exiting the stockpile, the thermocouple wires were bundled within a grounded steel conduit before entering the railway car that housed the logging computer. The thermojunctions were flame formed using an oxygen/acetylene torch and each was individually calibrated to a reference thermocouple and handheld thermocouple meter over the temperature range from 25°C to 100°C.

Advantech® automation hardware, PCL 818L in combination with four PCLD 789D computer automation cards, was used to monitor thermocouple voltages. Custom logging and control software, using Microsoft® Visual basic version 3.1, was initially developed to control the gas sampling and analysis operations as well as determine the thermocouple temperatures. Cold junction compensating algorithms were incorporated into logging software to account for the thermoelectric effects at the thermocouple termination point. 'PC ANYWHERE®' computer software was used to communicate to the logging computer from Sydney.

3.8. Moisture Determination.

The moisture profile across the 1.2m width of the stockpile was determined gravimetrically at selected times throughout the experiment. The bagasse sample was removed from the experimental stockpile using a custom manufactured 'coring' tool which resembled a large, power driven, version of the standard laboratory 'cork-boring' tool. A lathe was used to cut a sharp edge into one end of the 50mm diameter, 1.3m long, thin-walled steel tube. Welded to the other end of the tube was an attachment that allowed the tube to be rotated using a portable electric power drill. This attachment was partly removable and enabled a rod to be passed down the centre of the tube enabling the bagasse to be forced out of the tube. The length of the tube was also graduated at 100mm intervals.

The sampling procedure consisted of firstly cutting away a small section of the wire mesh sheet at the selected sampling position. A 1.2m length of bagasse was then cut from the stockpile parallel to, but at least 1m away from, the instrumented axis. Due to the tough fibrous nature of the bagasse, the coring tool could only cut to a depth 100 mm before friction overloaded the electric drill. Hence, twelve cutting operations were required to incrementally extract the entire 1.2m column of bagasse. After withdrawing each individual 100mm long core, the drill attachment was disassembled and a steel plunger inserted through the coring tool from the drill attachment end. The tightly packed bagasse sample was then pushed from the tube into a plastic bag and the bag quickly sealed. The moisture concentration was then promptly determined using the standard method described in section 2.4. Generally two cores were taken, one core taken at a distance of approximately 1.2m from the instrumented axis, the second core taken at several metres from the instrumented axis.

3.9. Results:

3.9.1. Self-heating behaviour of the 1.2m stockpile.

In this current section, the self-heating behaviour of the 1.2m stockpile for the period from December 1998 to October 2000 is discussed.

The bagasse sample was sourced from a local Mackay mill. Due to the reduced length of the 1998 sugar production season, it was necessary for the bulk bagasse sample to be delivered a number of days before the filling process could be commenced. Sub-samples of the bagasse were collected upon arrival and just prior to the stockpile filling, with the moisture content gravimetrically determined in the standard way. The moisture content was found to average 53.6% moisture on a wet basis with ~10% variation in moisture between the samples.

Figure 3.9.1 shows the temperature at five spatial positions for the first 400 days of the experiment. (Note that four thermojunctions were located at a distance 2m away from the instrumented axis and at a depth of 0.6m, that is, at a similar relative spatial position across the stockpile as the 0.6m instrumented axis thermojunction).

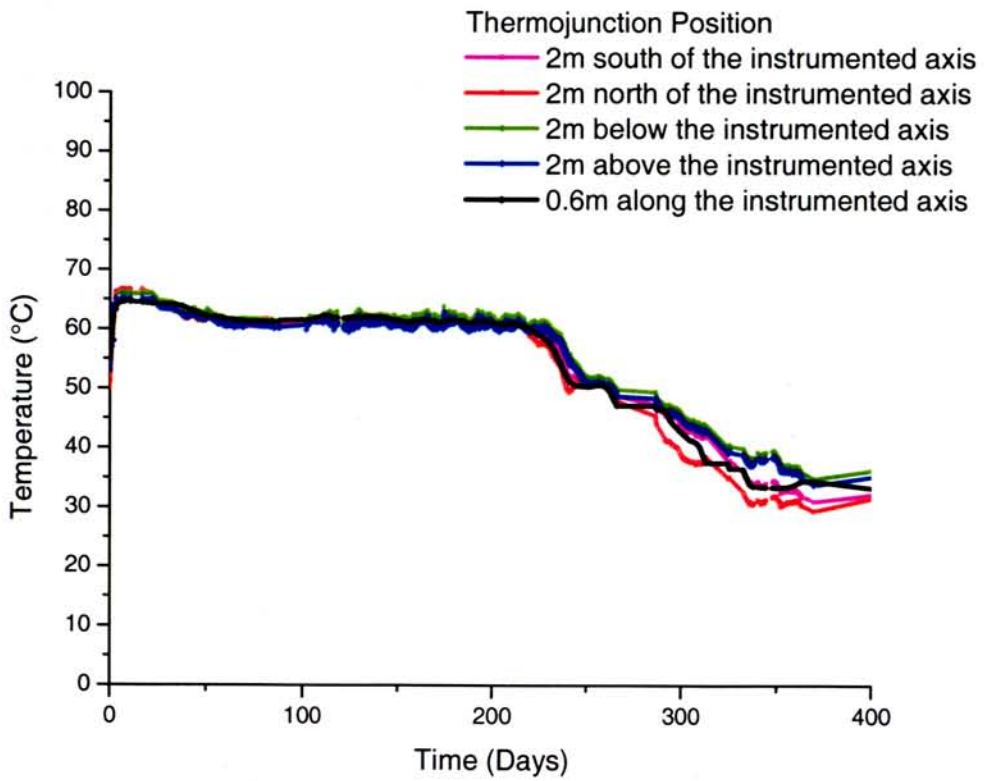

Figure 3.9.1: 0.6m temperatures of the 1.2m stockpile for the first 400 days.

Figure 3.9.1 shows good thermal homogeneity along the radial axes for a distance of at least 2m away from the instrumented axis position. These data show that the bagasse close to the instrumented axis experiences essentially no edge effects. These results verify that the bagasse sample near the instrumented axis is closely simulating the conditions that would be experienced within a true one-dimensional infinite slab of bagasse. As such, these data also vindicate the selection of radial stockpile dimensions of 8m.

From day 260 to approximately day 280, the Microsoft® Windows 95 computer operating system on the logging computer functioned unreliably. The computer was returned to Sydney and the Windows 95 computer operating system replaced with the Microsoft® Windows 3.11 computer operating system. During the period from day 370 to day 400, the UPS supply functioned unreliably and the computer 'hard disk drive' failed. Hence, it was required that the computer be returned to Sydney on a second occasion for repairs. Hence, over these periods, data has not been recorded.

Figure 3.9.2 shows the temperature history of the stockpile over the first 400-day period but this time showing the temperatures at 0.1m increments over one half of the instrumented axis. It should be noted that the coordinate system used to describe the measurements of the 1.2m wide stockpile are taken with respect to the eastern stockpile surface.

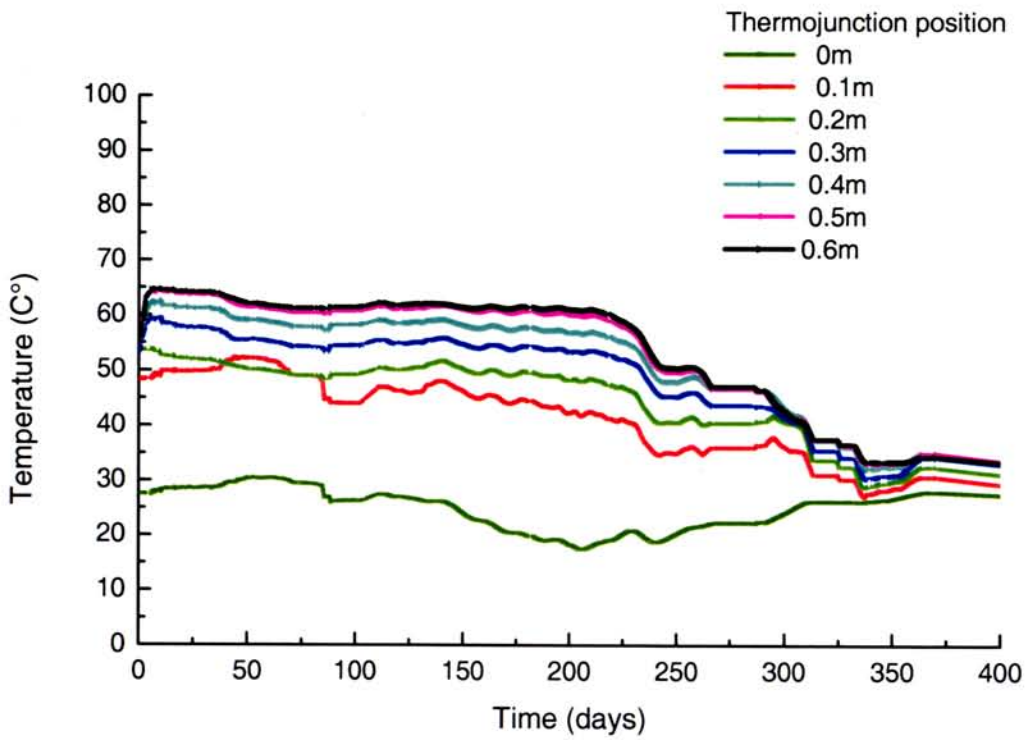

Figure 3.9.2: Temperature histories within the 1.2m stockpile at 0.1m increments over 400 days. Note that 0m refers to the stockpile surface.

The temperature at the 0m position represents the daily time averaged, surface temperature of the eastern side of the 1.2m stockpile. This temperature was measured by a thermojunction, embedded approximately 1cm into the bagasse on the eastern surface of the stockpile. The other traces represent the average daily temperature of a thermojunction located at the stated spatial position along the instrumented axis from the eastern face.

Figure 3.9.3 shows the temperature of the stockpile along the instrumented axis from the 0.6m to the western side of the stockpile.

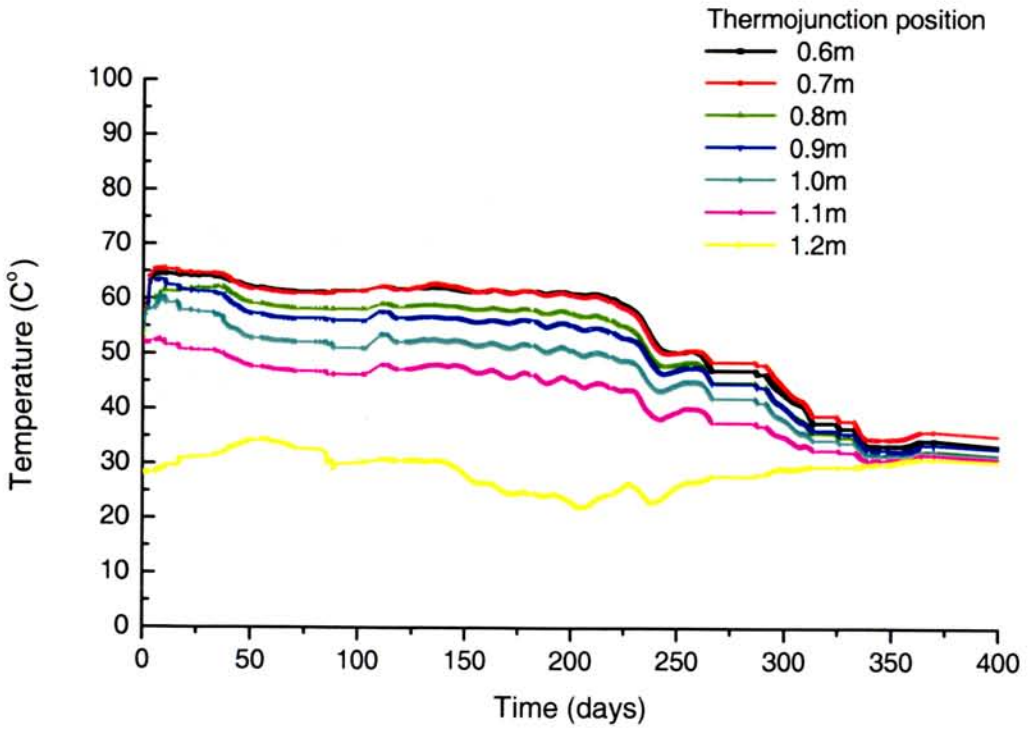

Figure 3.9.3: Temperature histories within the 1.2m stockpile at 0.1m increments from 0.6m to the western boundary surface for the initial 400 days.

The yellow trace in this data indicates the average daily temperature of the western surface of the stockpile while the black temperature trace indicated the temperature midway through the stockpile. Both figures 3.9.2 and 3.9.3 display a rapid initial increase in stockpile temperature which quickly increases to a maximum value of ~68°C within six days of filling. The stockpile then cools to an apparent steady state temperature of ~62°C after approximately 50 days. Once this apparent steady state was reached, the centre temperature of the stockpile remained essentially isothermal for a further 150 days. Notice that the centre stockpile temperature remains isothermal even though, the exterior average surface temperature of the stockpile drops by 12°C during the winter (or dry) season.

Figure 3.9.4 shows the increase in temperature of the stockpile above the surface temperature of the stockpile, which in this case is the western edge.

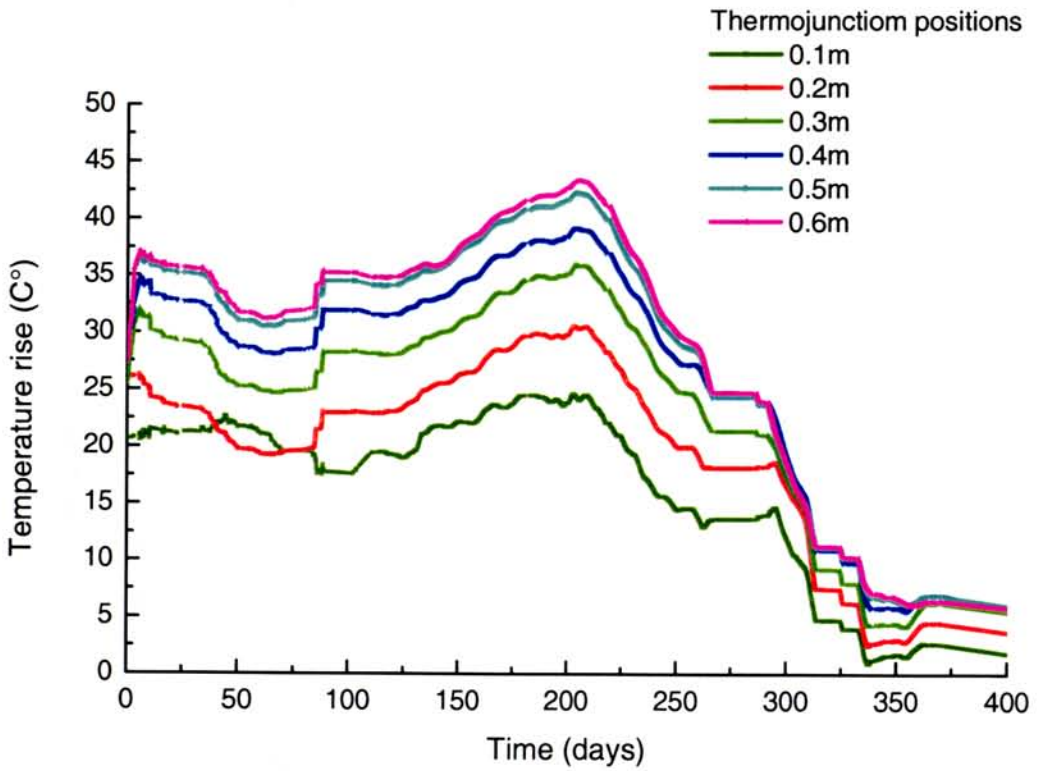

Figure 3.9.4: Temperature increase relative to the western side of the stockpile of the 1.2m stockpile at 0.1m increments.

These data clearly show an increase in the temperature gradient across the stockpile during the isothermal period from day 125 to day 220 and the rapid fall in temperature after day 220. These data show that the self-heating rate of the stockpile has increased and that the oxidation reaction has essentially 'switched off' at approximately day 220, suggesting that a significant change in the self-heating chemistry has occurred at this time. It is interesting to note that the increase in heat release rate has maintained the centre stockpile temperature close to 62°C.

Figure 3.9.5 displays four spatial profiles across the stockpile at day 70, 200 290 and 400.

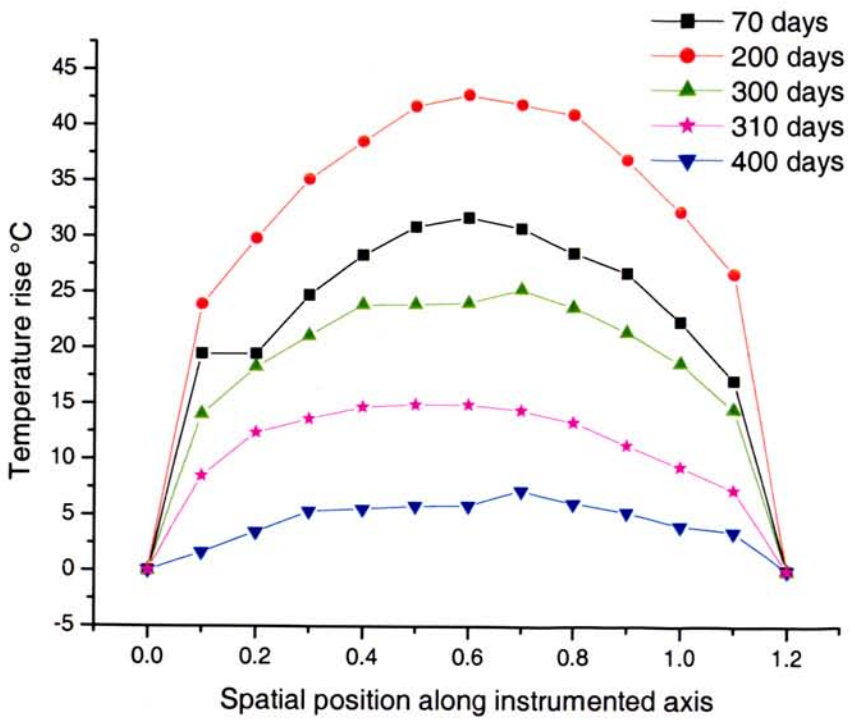

Figure 3.9.5: Temperature cross-section of the 1.2m stockpile at day 70, 200 290 and 400.

Figure 3.9.5 shows that the maximum temperature gradient within the stockpile exists over the initial 200mm thick surface layers of the slab. After the initial equilibration period, the temperature profile across the stockpile becomes approximately symmetric about the midpoint position, a feature that is shown by the temperature profiles at day 70 and day 200. These data suggest that the east/west orientation of the large stockpile has had little bias on the heating symmetry. Notice, however, that the temperature symmetry across the experimental stockpile becomes skewed towards the eastern side of the stockpile at day 310. The stockpile also becomes approximately isothermal between the 0.4 and 0.6m spatial positions suggesting that little self-heating is occurring at the centre of the stockpile.

Figure 3.9.6 shows the moisture concentration profile of the 1.2 m stockpile at 100mm increments at day 260 and day 330. The location where each core sample was removed from the experimental stockpile is shown in figure 3.9.6 (a).

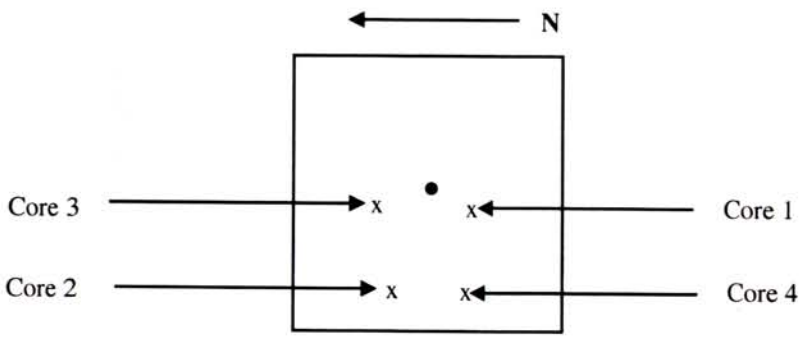

Figure 3.9.6(a): Sample locations for each core removed at day 260 and 330. The view of is from the western side

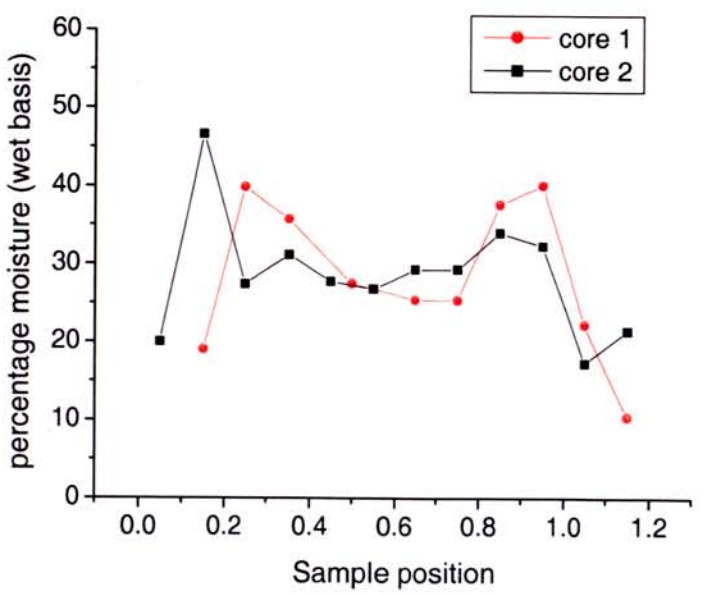

Figure 3.9.6(b): Moisture profile of the 1.2m stockpile at day 260.

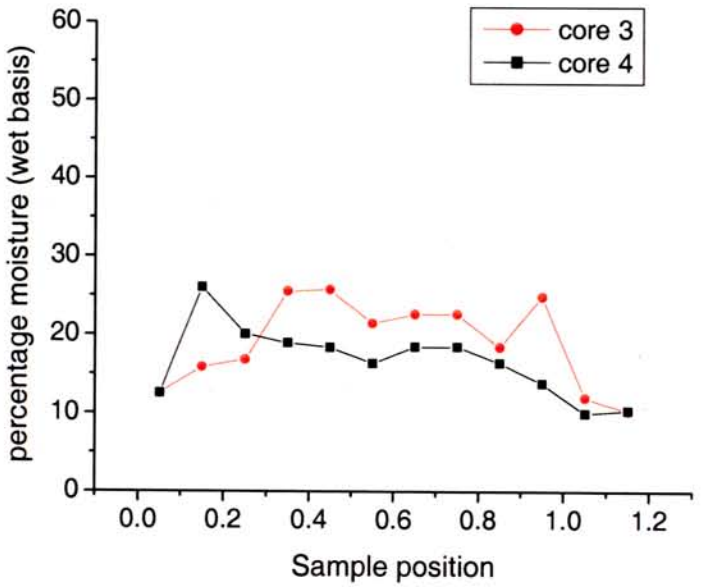

Figure 3.9.6(c): Moisture profile of the 1.2m stockpile at day 330.

Figure 3.9.6(b) shows that the average moisture content of the stockpile dropped from the initial average moisture value of 53% to approximately 25% at day 260. The similarity between the two samples shown in this figure suggests that moisture loss has occurred in an approximately uniform manner and that these data are representative of the stockpile as a whole. Figure 3.9.6(c) shows that the moisture loss continued as the stockpile progressively cooled and reached an average moisture concentration of ~20% (wet basis) at that apparent thermal minimum on day 330. These moisture profiles show a symmetric moisture concentration profile about the 0.6m position and further verify that the north/south orientation has not significantly influenced the self-heating behaviour. The generally lower moisture values at the centre of the stockpile suggest that the increased temperature at this position has driven moisture from the interior of the stockpile towards the cooler exterior surfaces, resulting in a maximum moisture concentration value at a depth of approximately ~0.3m.

Figure 3.9.7 shows temperature history plots from the centre of the stockpile to the western side of the stockpile, but this time for a 700 day period as well as the corresponding average rainfall over this period at time intervals of 4 weeks.

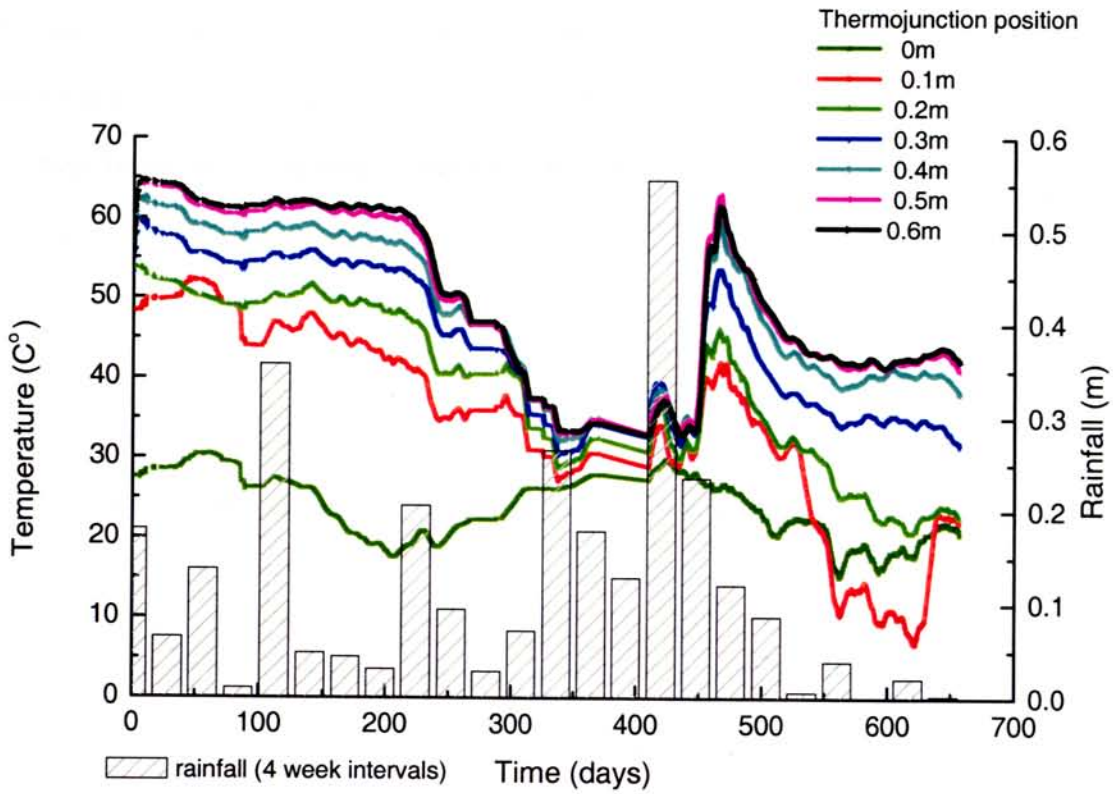

Figure 3.9.7: Temperature histories within the 1.2m stockpile at 0.1m increments from 0.6m to the western face and the corresponding local rainfall for Mackay for 4 week intervals.

(The rainfall data has been sourced from the Australian Bureau of Meteorology)

The main region of interest in figure 3.9.7 is the distinct temperature increase occurring at approximately day 460. The average rainfall data for Mackay is also shown. Notice the progressive increase in rainfall prior to the initial temperature rise at approximately day 420, with in excess of 0.5m of rainfall occurring during the three 4-week periods period leading up to the larger temperature rise. Notice also the correlation between the larger temperature rise at approximately day 460 and the very large amount of precipitation (in excess of 0.55m) that occurred approximately three weeks before this temperature rise. These data suggest that the prolonged rainfall over the preceding 100 days, combined with the large amount of rainfall at approximately day 420, was sufficient to reinitiate the wet oxidation reactions within the stockpile. As a result, the centre temperature of the stockpile increased by 28°C in 18 days. Following this temperature increase, the stockpile did not remain at the higher steady state temperature for the same extended period, as was the case after the initial filling of

the stockpile. It is suspected that the uneven rewetting of the stockpile is a result of a combination of both environmental factors, such as the prevailing wind and rainfall direction, as well as packing imperfections that developed as the stockpile consolidated. This latter factor, however, is more likely to be responsible for the moisture variation near the centre of the stockpile since packed bagasse tends to produce a heavily matted surface that inhibits water ingress. This is especially the case with vertical surfaces where water tends to run off the bagasse without penetration.

Figure 3.9.8 show the temperature profile through the stockpile at day 410, 421, 466 and 510.

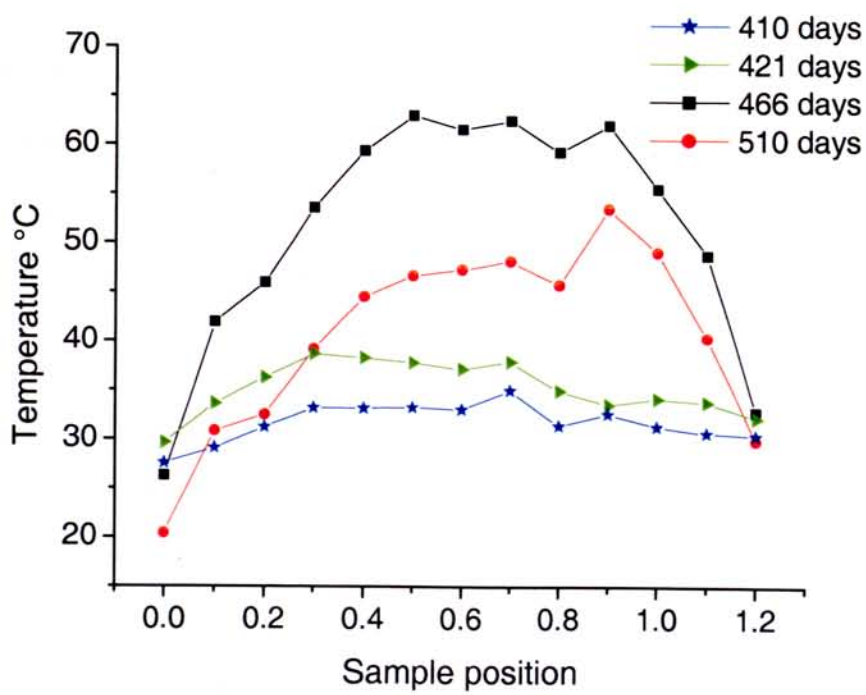

Figure 3.9.8: Temperature cross-section of the 1.2m stockpile at day 410, 421, 466 and 510.

These data shown in figure 3.9.8 display a generally less symmetric heating profile than that displayed in figure 3.9.6. This reduced symmetry is consistent with the corresponding moisture profile data, which is shown in figure 3.9.9, where the moisture profile of the stockpile at day 510 is displayed.

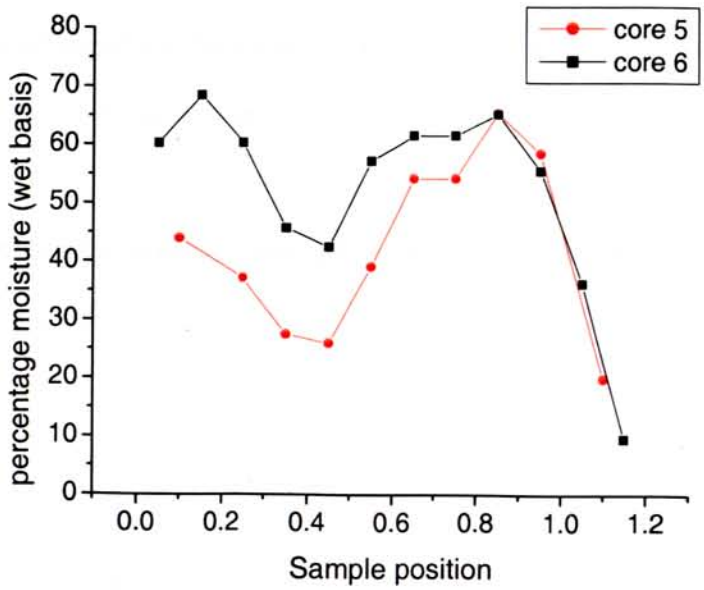

Figure 3.9.9: Moisture profile of the 1.2m stockpile at day 510

These moisture concentration data shown in figure 3.9.9 were taken from similar sampling positions to core 3 and core 4 that was shown in figure 3.9.6. In this current figure, core 5 was located closest to the instrumented axis. Notice that the moisture profile in figure 3.9.9 is skewed towards the 1.2m sample position and partially reflects the temperature profile of figure 3.9.8.

These current moisture concentration data, however, show an increased variation between the samples as compared to the data shown in figure 3.9.6. These results suggest that the stockpile has not been uniformly moistened, with the eastern side of the stockpile (sample position 1.2m) displaying a significantly greater spatial moisture concentration variation than that of the western side. It is suspected that the uneven rewetting of the stockpile is a result of a combination of both environmental factors, such as the prevailing wind and rainfall direction, as well as packing imperfections that develop as the stockpile consolidates. This latter factor is suspected to be mainly responsible for the moisture variation near the centre of the stockpile since packed bagasse tends to produce a heavily matted surface that inhibits water ingress. This is especially the case with vertical surfaces where water tends to run off the bagasse without penetration. Given the possible inhomogeneity in stockpile rewetting, combined with the probability that the bagasse may be chemically different following over 12 months of decomposition, it is not unexpected that the stockpile did not remain at the quasi steady-state temperature for a similar period to the initial steady state period. Clearly, further experimental

research is needed regarding the chemical processes that occur within bagasse stockpiles before this experimental data can be fully understood.

Figure 3.9.10 shows the moisture corrected oxygen, carbon dioxide and nitrogen concentrations at the centre of the stockpile.

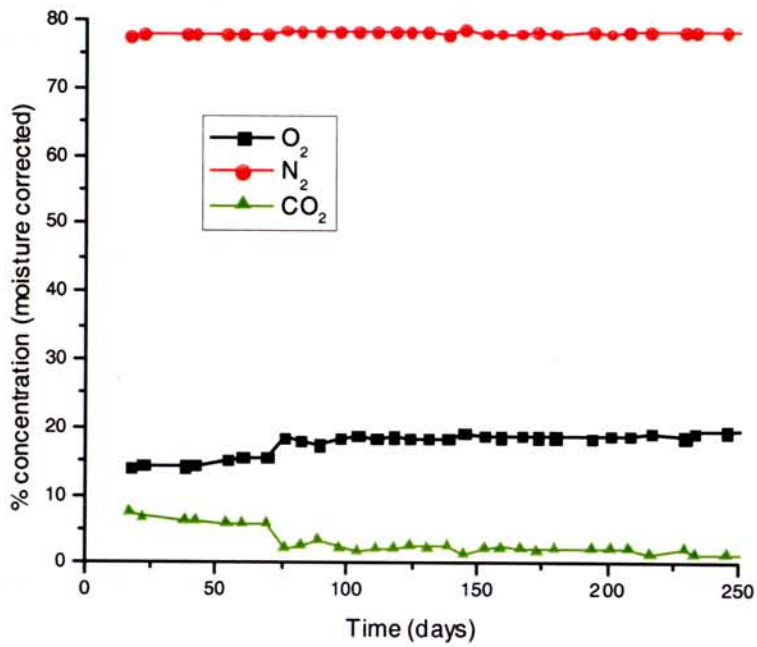

Figure 3.9.10: Variation in permanent gas concentration at the centre of the 1.2m stockpile for the first 250 days.

The general behaviour of the data presented in the above figure, are consistent with the behaviour of this material during laboratory oxidation measurements where bagasse samples also display an initially high oxygen deficit and CO_2 concentration that both relax to a steady state value after approximately 150 days. Notice that the CO_2 concentration is inversely coupled with the oxygen deficit, a behaviour that is consistent with laboratory experiments. The measurements also showed that the CO concentration was less than ~2000ppm, which was the limit of resolution of the GC used.

3.9.2. Self-heating behaviour of the 0.5m wide stockpile

During this study the 0.5m stockpile was filled twice. During the first filling, the same loading method as used to fill the 1.2m wide stockpile was also used to fill the 0.5m wide stockpile. Hence, by using a common packing method, it was expected that the loading density and packing characteristics of both stockpiles would be similar. While the exact density of each stockpile was not known, the mass of bagasse (as approximated by the crane operator from observations of the crane's load cell readings) loaded into each stockpile suggested that this assumption was correct. Following this initial filling, the 0.5m wide stockpile, however, cooled quickly to a temperature of only a few degrees above ambient air temperature. Upon disassembly many months later, it was found that the stockpile was dry, lightly packed and contained large voids that allowed the free flow of ambient air through the stockpile. A detailed investigation revealed that the fibrous nature of the bagasse, in association with the surface structure presented by wire mesh, allowed the bagasse to bind to the mesh and form self-supporting layers that spanned between the opposing mesh sides of the cage. Due to the strength of these layers, which could nearly support a 75kg mass, the bagasse did not uniformly move downward as the material consolidated resulting in a network of open voids throughout the stockpile. This problem did not occur with the 1.2m wide stockpile due to the increased width and bagasse mass. Since the consolidation problem could not be overcome without a significant redesign of the cage, the objective of this experiment was modified. It should also be noted that after the first filling of the 0.5m wide stockpile, the appearance of the bagasse packed within this stockpile was visually identical to bagasse that was packed within the 1.2m wide stockpile. Furthermore, due to the large distance to Mackay (1500km), the consolidation problem of the 0.5m wide stockpile was not detected until the stockpile was re-inspected several months later.

It was proposed that insulating one or more sides of a much smaller stockpile could be an economically viable alternative method for constructing simulation stockpiles that could be used for model validation. To investigate the effectiveness of this proposal, a 50mm thick layer of polystyrene insulation was installed onto the southern 5m x 5m surface of the 0.5m stockpile. While it was anticipated that the consolidation problem would persist, since the construction of the cage was

unchanged, it was hoped that some information would be gained regarding the performance of this technique.

During this second filling of the 0.5m wide stockpile a modification to the first filling method was used. In this second method, the bagasse was manually lifted and packed into the cage in small quantities to improve the packing uniformity of the stockpile. It was also expected that this revised packing method would also produce a slight increase in stockpile density. To form an intimate bond between the bagasse and the foam surface, polyurethane foam was injected into the cavity between the bagasse and the surface of the sheeting, effectively sealing this bagasse surface to air, moisture and heat transfer. The temperature of the bagasse at the time of loading was at approximately 21°C and for this current study, the stockpile was instrumented with thermocouples only. The 0.5m wide stockpile insulated with a layer of polystyrene foam, is shown in figure 3.9.11.

Figure 3.9.11: The 0.5m stockpile insulated with polystyrene foam. The red painted steel conduit (shown in the foreground of this figure) was used to protect and convey the bundled data wires from both the 1.2m and 0.5m stockpiles (located to the left of this figure) to the rail car that housed the logging instrumentation.

The heating behaviour displayed by the 0.5m stockpile following the second filling is shown in figure 3.9.12

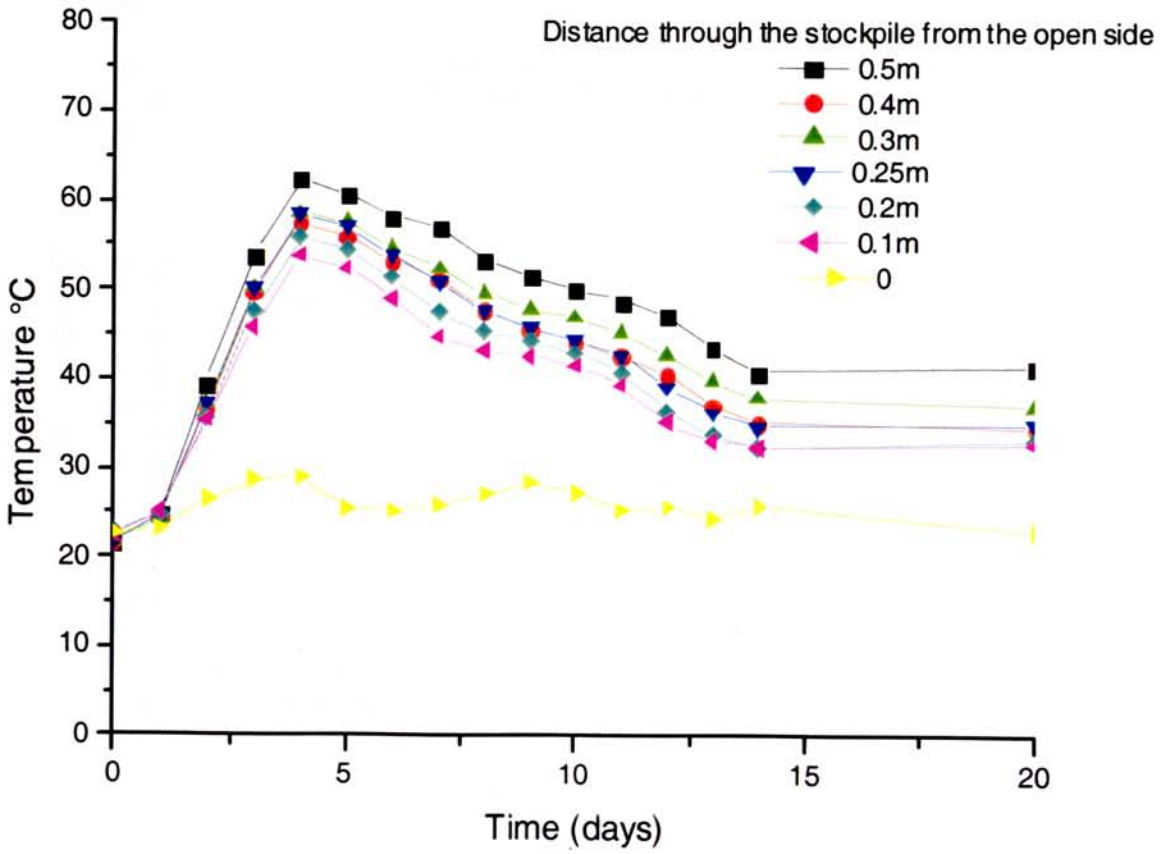

Figure 3.9.12: Temperature histories within the 0.5m wide stockpile for the first 20 days following the second filling.

These data displayed in figure 3.9.12 show very good agreement with the initial heating behaviour of the 1.2m stockpile, with the current data reaching a maximum temperature of 62°C in 4 days, while the data for the 1.2m stockpile reveal a maximum temperature of 62°C being reached in approximately 10 days. As shown in the above figure, the stockpile could not maintain the maximum temperature, a result that has been again attributed to the consolidation problem that has been identified previously.

The heating profile for the 0.5m stockpile is compared to the heating profile of the 1.2m stockpile in figure3.9.13.

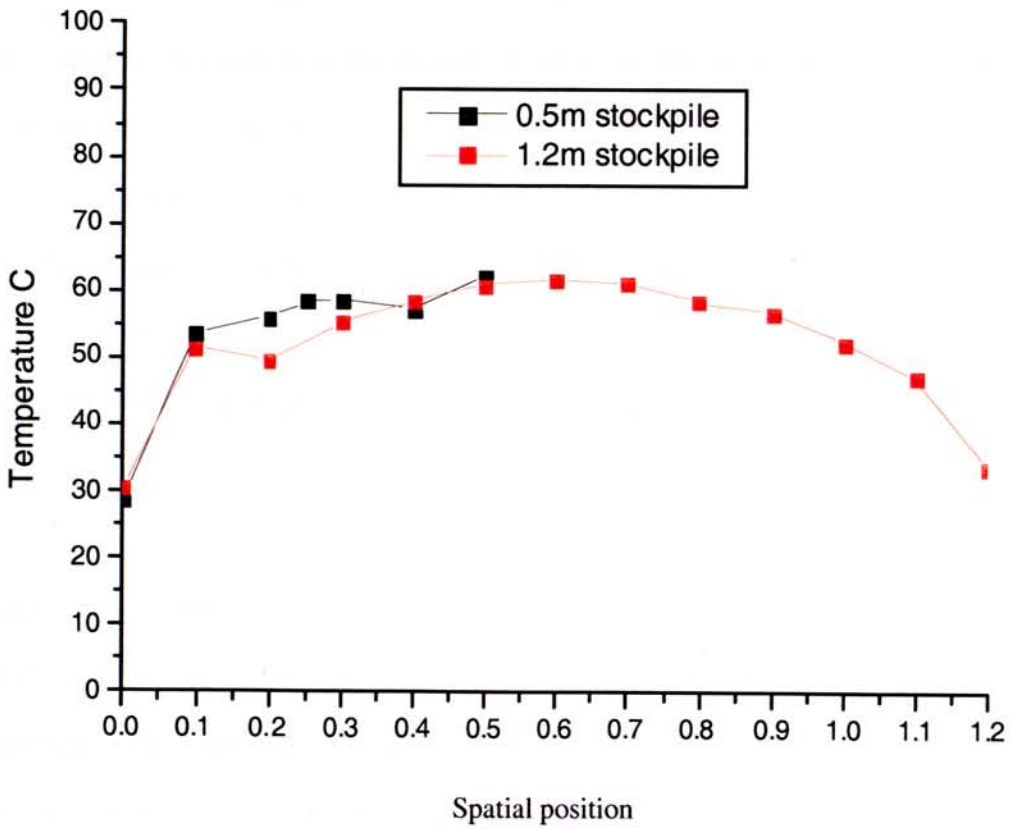

Figure 3.9.13: Comparison between the temperature profile of the 0.5m wide and the 1.2m wide stockpiles.

Figure 3.9.13 shows the temperature profile of the 0.5m wide stockpile at a time of 4 days and the 1.2m stockpile at a time of 10 days. The thermoelectric junctions for both sets of results are located along the instrumented axis. The profiles displayed by these two data sets show good similarity over the region of interest and suggest, that the 0.5m insulated stockpile is simulating a much larger body. This agreement is even more striking when one also considers that the 1.2m wide stockpile was aligned in an east/west direction while the smaller stockpile was aligned along a north/south direction. Clearly, the method whereby one or more sides of a body are insulated to simulate the behaviour of larger sized body, has significant potential from an economic perspective.

3.9.3. Self-heating measurements upon higher density stockpiles.

This section describes two further studies that were aimed at examining the density dependence of the self-heating behaviour of bagasse. Ideally, to obtain results that are directly comparable to the data shown in section 3.9.1, that is, where the only differing variable is that of bagasse density, one would refill and monitor the 1.2m wide experimental stockpile (section 3.9.1) with bagasse at an increased or reduced density. Budgetary restraints, however, deemed that the most expedient method to investigate the density dependence would be to assemble the experimental stockpiles from high-density bagasse bales. As an extension of this experiment, the effectiveness of insulation for simulating a much larger stockpile was further examined, in this case with a single bagasse bale insulated on the four radial surfaces.

The bagasse bales used in this current study were sourced from a sugar mill located near Townsville Queensland. To eliminate moisture loss during the journey, each bale was individually shrink wrapped in polyethylene film. Figure 3.9.14 shows two of the bales wrapped in plastic film while figure 3.9.15 shows the assembly of the 9 bales of bagasse that were used to form a 1.1 m wide experimental stockpile. Just prior to the assembly of each stockpile, the polyethylene film was removed from the bales.

Figure 3.9.14: Two of the polyethylene film wrapped bales of bagasse.

Each bale, when viewed as shown in figure 3.9.14, had a height of 1.1m a width of 0.78m and a length that varied depending upon the mass of bagasse that was loaded into the bale forming press. The mass

Each bale, when viewed as shown in figure 3.9.14, had a height of 1.1m a width of 0.78m and a length that varied depending upon the mass of bagasse that was loaded into the bale forming press. The mass of bagasse packed into each separate bale was variable and produced bagasse bales with lengths ranging from 1.2m to 1.7m. The instrumented bale located at the centre of the assembly possessed a length of 1.65m and a density of 546kg/m^3 at the time of assembly.

Figure 3.9.15: The 'infinite' slab assembly simulation of nine bagasse bales.

The simulation shown in figure 3.9.15 was formed by tightly stacking each of the nine bales on its 1.1m wide side. In the above figure, the centrally located bale was instrumented with nine thermojunctions. The centre bale also displays a slightly darker surface than the corresponding perimeter bales, a result of additional surface moisture at the centre bale compared to the perimeter bales at that time. This occurred due to the recent removal of the polyethylene film covering the exposed surfaces as compared to the perimeter bales, where the film had been removed several hours earlier. Hence, the surface moisture concentration of the centre bale was slightly greater then that of the perimeter bales, a feature that disappeared as the bale dried in the subsequent few hours. This current figure also shows the position of the instrumented axis (Z) where six thermojunctions were installed at equally spaced intervals. Figure 3.9.15 also shows areas where pressure injected

Figure 3.9.16 shows the temperature history of the 1.1m wide assembly of bagasse bales.

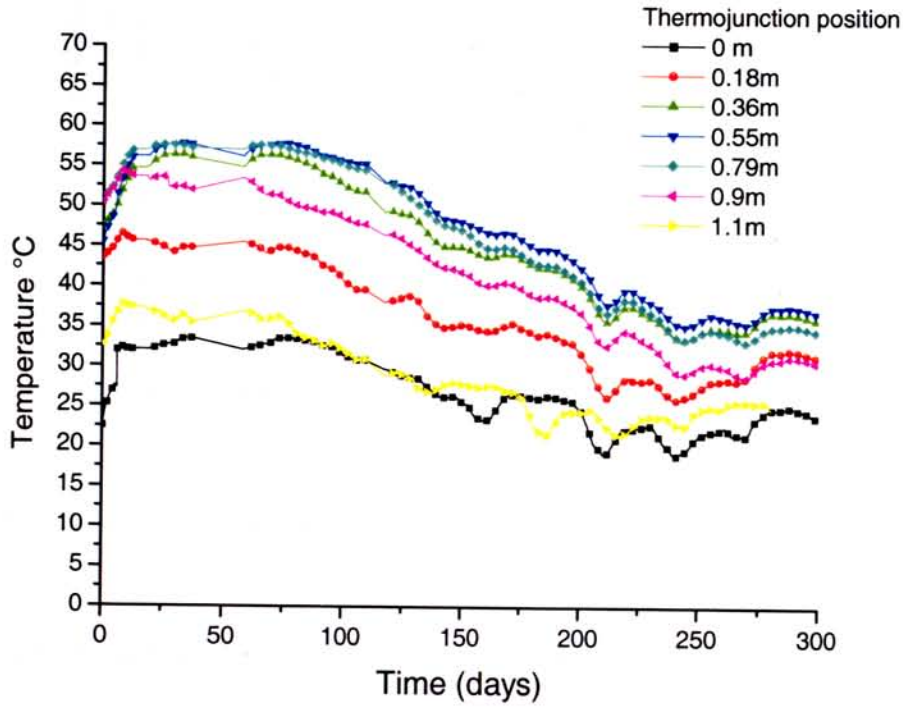

Figure 3.9.16: Temperature history of the 1.1m wide assembly of bagasse for a period of 300 days.

The above figure exhibits a self-heating behaviour that is generally similar to the behaviour displayed by the 1.2m wide stockpile with the temperature of this current stockpile increasing rapidly to a constant temperature after assembly. In this case, the stockpile heats to and maintains a temperature of 57°C for approximately 60 days before reducing to a lower temperature that is approximately 10°C greater than ambient air temperature. It should be noted that over the final 100 days of this experiment, the bales surrounding the instrumented stockpile progressively crumbled and by the end of the experiment, the perimeter bales were significantly eroded. While the instrumented bale was essentially intact at the conclusion of the experiment, the data over the final 100-day period require careful interpretation.

The moisture concentration of the instrumented bale was determined at 100mm increments along the instrumented axis. Two repeat determinations were completed, the results of which are shown in figure 3.9.17.

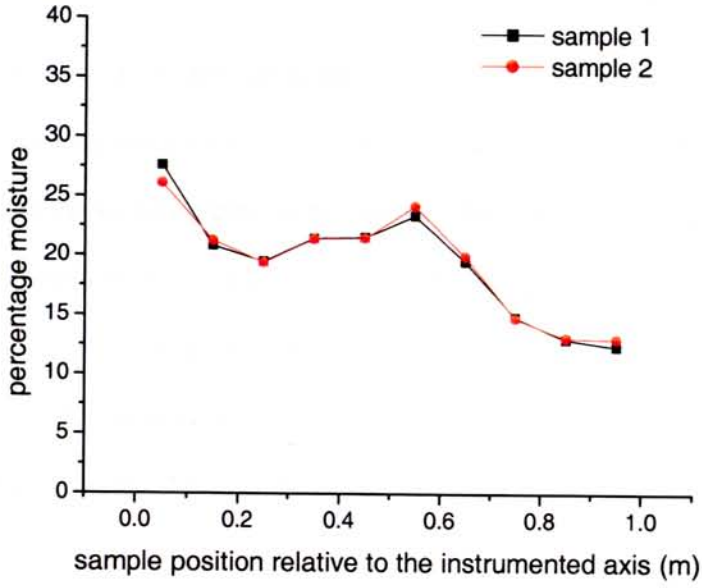

Figure 3.9.17: Moisture profile along the instrumented axis at day 300.

These data presented in figure 3.9.17 show significant asymmetry compared to the corresponding symmetric moisture profile of the 1.2m slab and suggest non-uniform moisture transport has occurred.

Figure 3.9.18 shows the corresponding temperature profile at day 300.

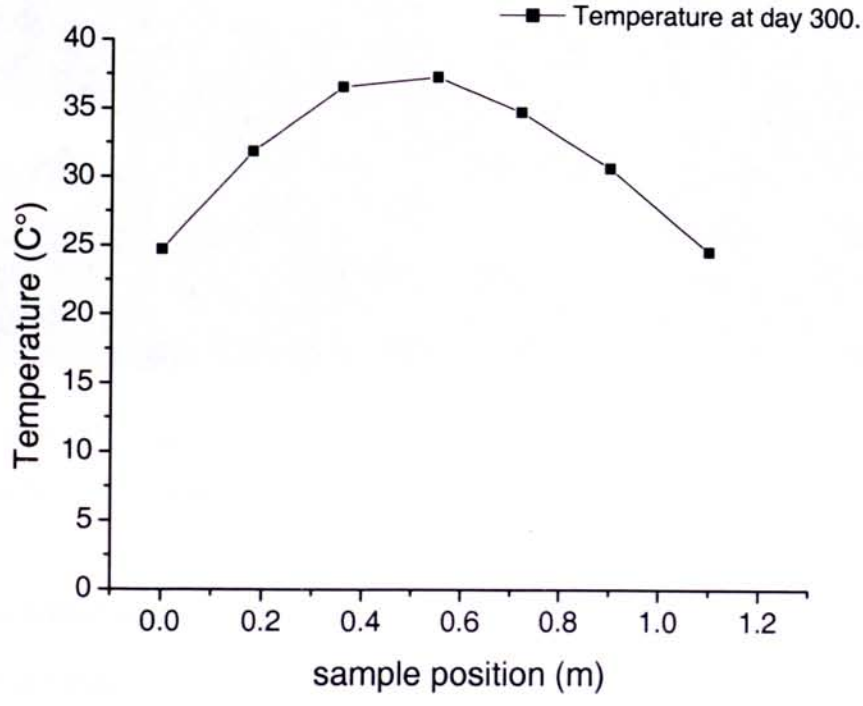

Figure 3.9.18: Temperature profile along the instrumented at day 300.

Comparing the moisture data of figure 3.9.17 and the temperature data of figure 3.9.18, the relationship between the two sets of data is not clear. While the above temperature profile agrees somewhat with the moisture data with respect to the bias towards the 0.0m position, the distinctive moisture minimum at the spatial position of the temperature maximum that was displayed in the previously presented data of the 1.2m wide stockpile is not evident in this current data. (The author would like to thank the staff at SRI for completing the final moisture measurement of the stockpiles and form undertaking the disassembly and clean up of the stockpiles)

A novel inclusion to this current study was also completed to evaluate the effectiveness of insulating four sides of a bagasse bale to simulate a much larger body. A single bagasse bale with dimensions 1.65m x 0.78m x 1.1m was instrumented with six thermoelectric junctions and then insulated with a 50mm thick layer of polystyrene foam on each of the 1.65m and 0.78m sides. The bagasse bale is shown in figure 3.9.19.

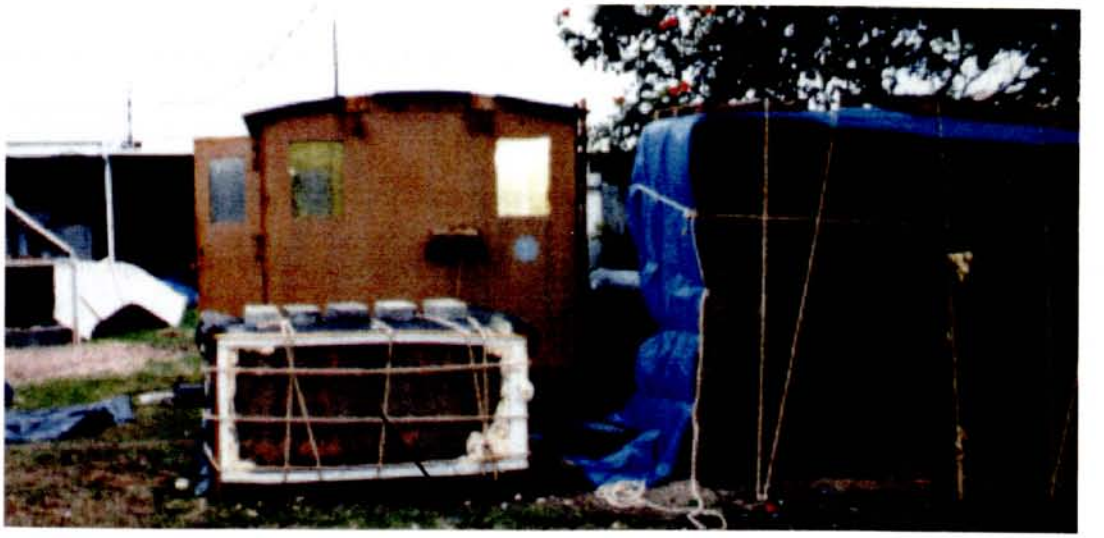

Figure 3.9.19: The single insulated bale of bagasse. The plastic sheeting used to seal the assembly of bales from the vertical ingress of rainwater is also shown in this figure.

The instrumented axis, along which six equally spaced thermoelectric junctions were positioned, is identified in figure 3.9.19 as the 'Z' axis. A shown this figure, the 'Z' axis is aligned parallel to the

four insulated sides of the bagasse bale and passes through the centre of the two 1.65m x 0.78m wide surfaces. At the time of the construction the above bale possessed a density of 530kg/m^3.

Figure 3.9.20 shows the temperature history of the 1.1m insulated bale of bagasse.

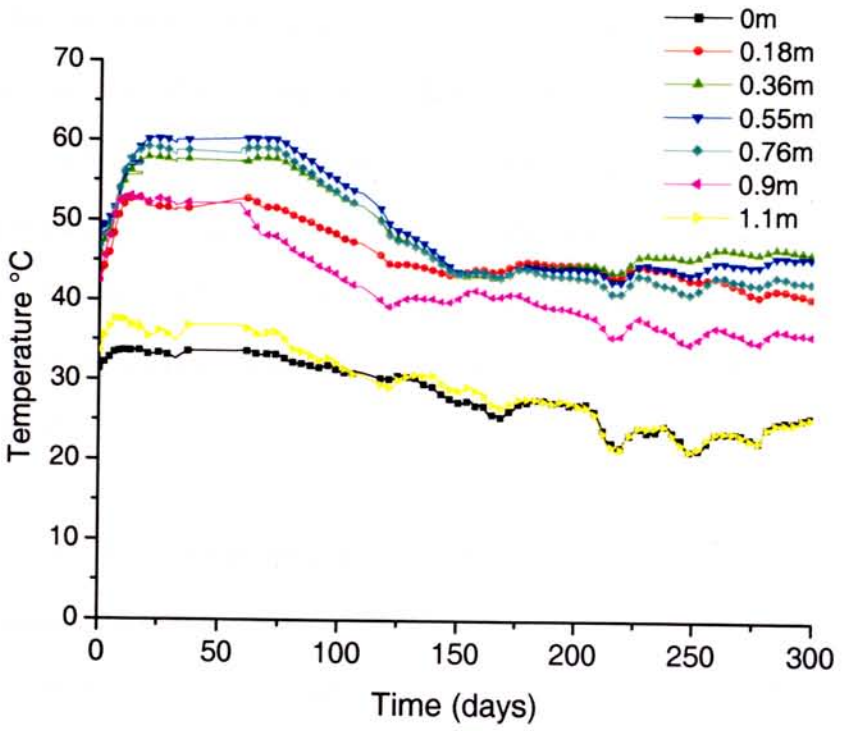

Figure 3.9.20: Temperature history of the 1.1m wide insulated bale of bagasse for 300 days.

Figure 3.9.20 shows a similar temperature history to that of the assembly of the nine bagasse bales. In this current figure, the average temperature over the steady state period was 62°C with the stockpile remaining at this temperature for 60 days. Also, notice that after reaching a minimum temperature of 44°C at approximately day 150, the maximum temperature of the bale slowly increased over the next 150 days, an aspect that will be discussed later in this chapter.

3.10. Discussion

3.10.1. Comparison with published data

The bagasse stockpile behaviours examined in this thesis are consistent with other published measurements. Dixon (1988) has reported temperatures of commercial bagasse stockpiles at number locations in Queensland Australia. In this study, measured temperatures at a depth of 0.5m ranged from 48 to 60°C, which is consistent with the findings of the current study. During further experiments completed by Dixon (1988) and Ashbolt (1986), the temperature of smaller stockpiles, which had been treated with biocide, were measured. In that study, measurements were completed on small stockpiles (cones 2.5m high, 3.5m diameter) that had been treated with biocide and one 'control' stockpile that was untreated. In all cases the stockpiles behaved similarly and self-heated to temperatures between 60 and 65 °C.

Gray et al (1984) has reported that the centre temperature of critical ambient temperature tests is held on a plateau over the temperature range between 50 and 80 °C depending upon the packing density. While this study is experimentally quite different to the current work, the authors attributed the findings to water movement within the bagasse sample which suggests that this may be linked to the observations of the current study.

3.10.2. Discussion and comparison of the Experimental results of this chapter to the Theoretical results of Macaskill, Sexton and Gray (1998)

While the experimental results of this current chapter may be discussed as an independent experimental study of bagasse self-heating within stockpiles with simple geometry, it is instructive to compare the findings of this current chapter with predictions of Macaskill, Sexton and Gray (1998). The most current formulation of the model, that includes variables such as reactant consumption, oxygen concentration and more complex stockpile geometry, are examined for one-dimensional stockpile geometry. It should be emphasized that that the model calculations discussed in this section have been kindly undertaken by Dr Jane Sexton and are not the work of the author of this thesis. The reader is referred to the original publications (Macaskill, Sexton and, Gray 1998, Gray, Sexton, Halliburton and Macaskill, 2001) for a full description of the model and its formulations. Other than the specific calculations completed by Dr Jane Sexton at the request of the author of this thesis, the

computational results discussed in this section originate from the above publications. Additionally, it should be noted that this current field study is concerned with self-heating phenomenology rather than the transition of self-heating to ignition, with the stockpile dimensions used in this study being chosen to reflect specific self-heating behaviour that could be readily modelled. Given the stockpile dimensions it was also not expected that the stockpile would proceed beyond self-heating to "self-combustion".

The simulated data in this current section have been calculated using an initial bagasse temperature of 55°C, an initial moisture concentration of 50% (wet basis) and a constant ambient air temperature of 30°C. The initial temperature and moisture values were chosen to reflect the approximate initial conditions of the bagasse sample at the time when it was loaded into the 1.2m wide stockpile. The water vapour concentration within the stockpile was assumed to be in equilibrium with the bagasse liquid water phase while the external relative humidity was assigned a value of 70%, which corresponds to humidity conditions typical of the north of Queensland, Australia. The density of the experimental stockpiles is the least well-known parameter, but is generally between 100 and 190kg/m^3. For the computer experiments a density value of 125kg/m^3 was assumed. The calculated temperature and moisture loss behaviour of a 2.2m wide bagasse stockpile, as well as temperature behaviour of the 1.2m wide experimental stockpile, are shown in figure 3.10.1 for the initial 400 day period.

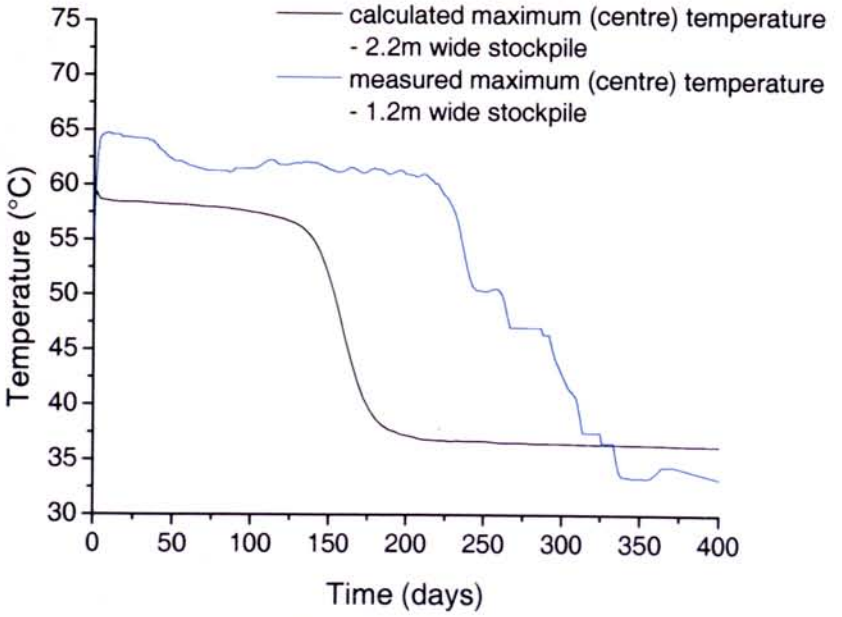

Figure 3.10.1: Temperature history of the 1.2m experimental stockpile at a depth of 0.6m and the calculated history of a 2.2m bagasse for 400 days.

The calculated data shown in figure 3.10.1 predicts that a 2.2m wide stockpile would heat to an apparent steady state temperature of approximately 60°C. This state will be referred to as the quasi-steady-state. It is further predicted that the stockpile would remain at the quasi-steady-state temperature for an extended period and then quickly cool to a temperature slightly above ambient temperature. A comparison of the main features of both the calculated and the experimental data show that the main thermal behaviour of the 1.2m wide experimental stockpile has been captured by the model, with both the quasi-steady-state condition followed by the period of rapid cooling being predicted. This is particularly noteworthy given the complexity of the bagasse chemistry, the uncertainty in the magnitude of the bagasse density and the environmental conditions experienced by the experimental stockpile compared with the assumptions of the model calculations. This broad agreement is further reflected in the initial heating data shown in figure 3.10.2, where the temperature history for the first five days are shown for both sets of data.

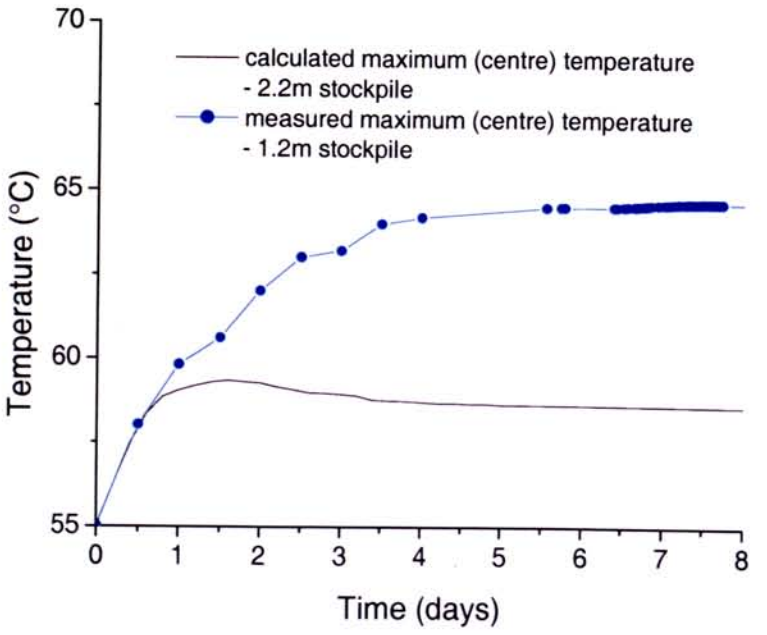

Figure 3.10.2: Experimental and calculated temperature for a 2.2m theoretical and the 1.2m stockpiles for the initial 8 day period..

The experimental data displayed in figure 3.10.2 shows that after stockpile formation, the stockpile temperature quickly increases from the initial temperature of 50°C to the quasi-steady-state temperature. While the maximum temperatures attained by each stockpile as well as the quasi-steady-state temperature are different for each case, the initially rapid heating rate of the experimental data is reflected in the calculated data.

Figure 3.10.3 shows that the quasi-steady-state is constant with respect to temperature only, with the moisture concentration within the stockpile gradually reducing in response to moisture being lost to the atmosphere at the bagasse surface.

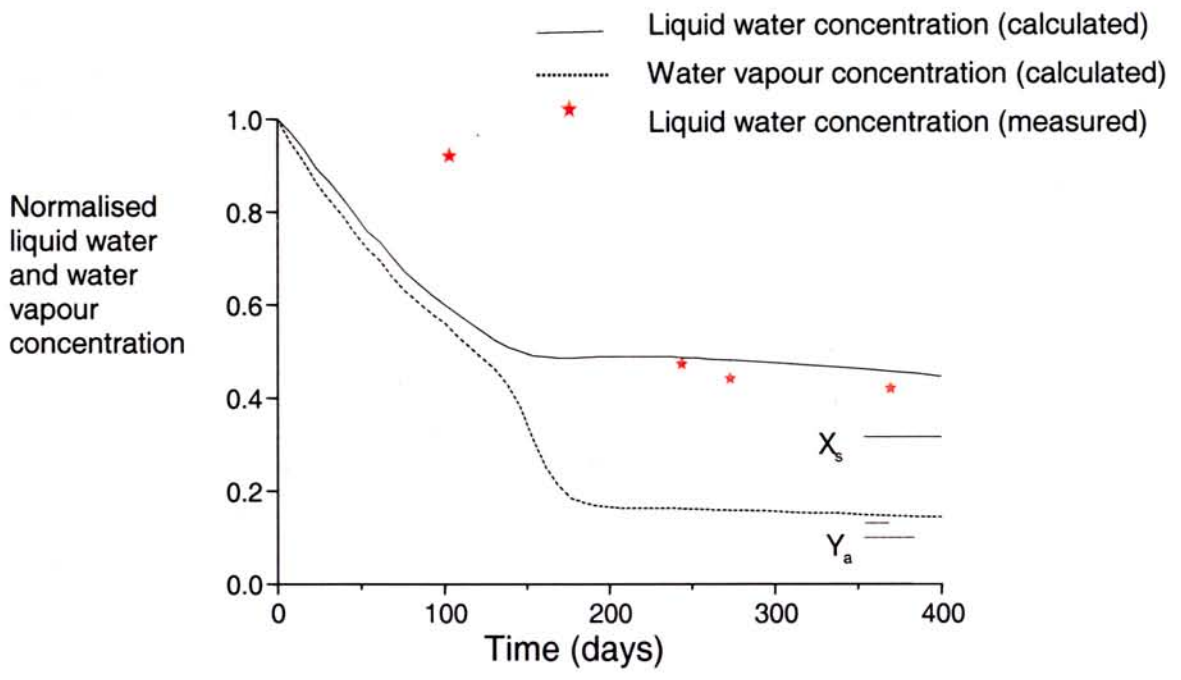

Figure 3.10.3: Calculated water vapour and liquid water history of a 2.2m bagasse for 400 day and measured experimental stockpile moisture concentrations. (Note that the concentration units have been scaled relative to the initial concentration values).

Figure 3.10.3 shows that after approximately 200 days, the liquid water concentration has been reduced by evaporation and diffusion processes to a value that is insufficient to sustain the wet oxidation reactions within the bagasse, resulting in the relatively rapid cooling of the stockpile. This phenomenon represents an 'extinction bifurcation' of this self-heating system after which, the liquid and water vapour concentrations approach their true steady state values. The calculated true steady state concentrations for the liquid water and the water vapour are shown as (X_S) and (Y_a) respectively. Other than at the initial time of filling, the bagasse liquid water concentration was not determined prior to the bifurcation event, however, the calculated data display a good agreement with the experimental data after the event.

The corresponding calculated liquid and water vapour concentrations for the first 5 days are shown in figure 3.10.4.

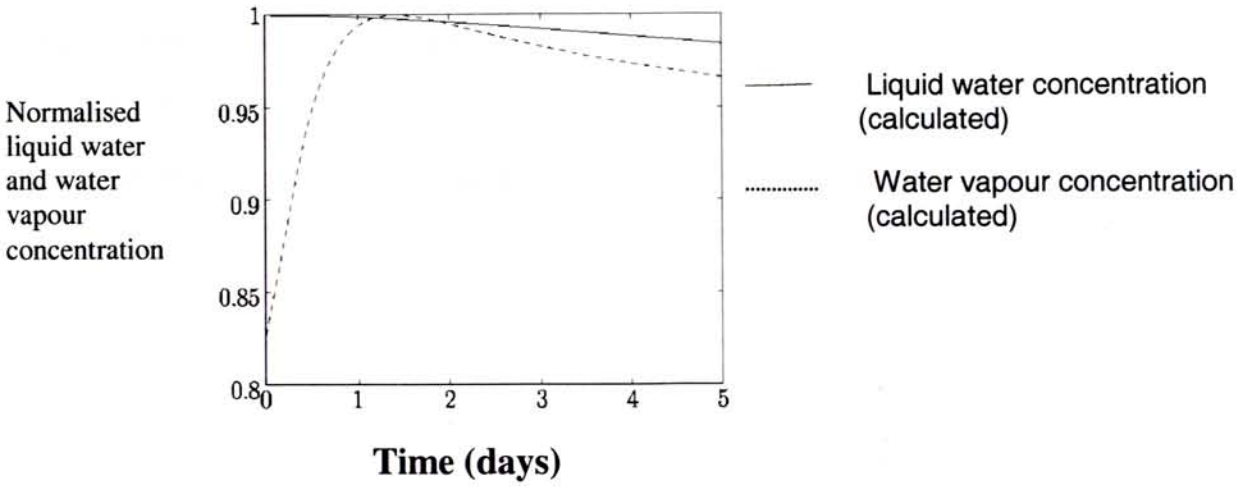

Figure 3.10.4: Calculated water vapour and liquid water concentrations for a 2.2m theoretical bagasse stockpile for a period of 5 days. (The water vapour data is shown as the dotted line.).

These calculated data suggest that the water vapour phase would quickly adjust to achieve a quasi-steady-state condition, while the liquid water concentration would slowly decrease due to stockpile drying.

Figure 3.10.5a shows the spatial evolution of temperature over the initial rapid heating period for both the experimental and theoretical experiments.

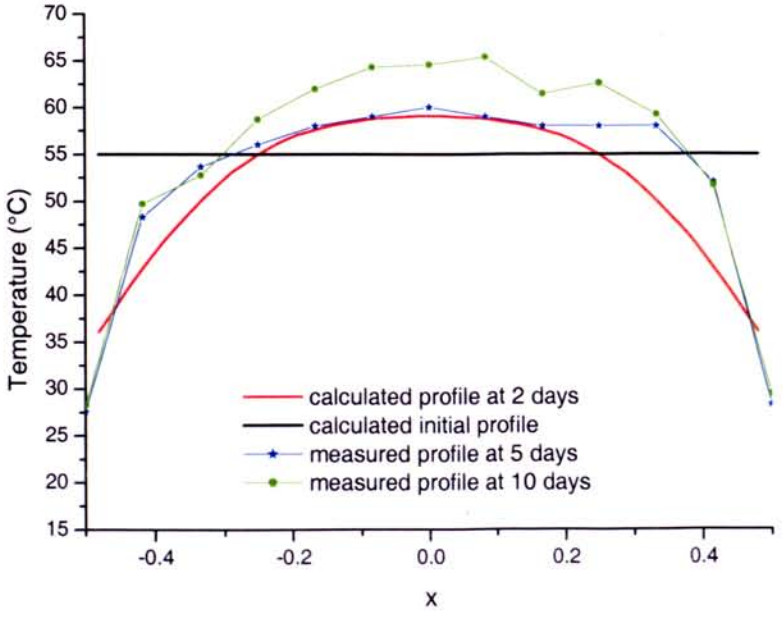

Figure 3.10.5a: Spatial temperature profiles for the experimental 1.2m and theoretical 2.2m stockpile over the initial rapid heating period.

Figure 3.10.5a shows the development of a parabolic spatial temperature distribution across the width of the slab. The calculated data suggest that the parabolic dependence would develop quickly from the initial isothermal condition at the time of construction and persist whilst the stockpile remains at the quasi-steady-state temperature. Since the temperature of bagasse at the time of construction of the 1.2m wide stockpile was at a temperature of approximately 55°C, this temperature was utilized as the initial temperature for these calculations. (It should be noted the 55°C is also the approximate temperature of the bagasse at the time of stockpile construction at commercial sugar mills.) While the temperature during the formation of the 1.2m wide stockpile was not measured, it would be reasonable to assume that the 1.2m wide stockpile would be relatively thermally homogeneous just following the loading of the cage. Hence, a constant temperature profile was used for theses calculations as this was considered the best approximation of the initial conditions of a quickly assembled stockpile. Using this assumption, the calculated temperature profile development is supported by the experimental data with a nearly circular temperature profile developing by day 2 and a parabolic profile developing by day 10. This increase in curvature of the temperature profile is consistent with an initial temperature profile being thermally homogeneous.

Figure 3.10.5b shows the same spatial evolution of temperature but this time from day 130 to day 200.

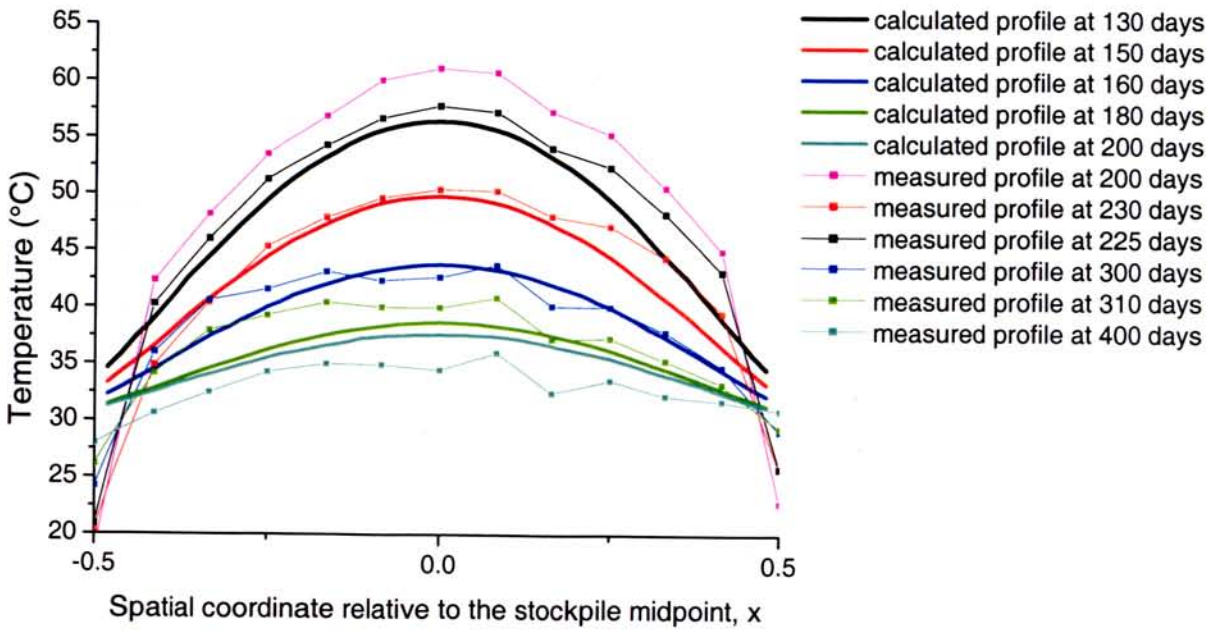

Figure 3.10.5b: Spatial temperature profiles for the experimental 1.2m and theoretical 2.2m stockpile over the initial rapid heating period.

In the above figure, the temperature profiles displayed have been selected so that the experimental and theoretical profiles are approximately comparable relative to the extinction bifurcation event that occurs within each data set. Both sets of temperature profiles remain generally symmetric about the midpoint position suggesting that moisture has been lost equally through each side of the stockpile. Clearly, for this experimental case, these data demonstrate that the model has captured the spatial self-heating behaviour of the 1.2m wide experimental stockpile.

Since the model assumes that the water vapour within the stockpile is in equilibrium with its liquid phase, the calculated vapour phase concentration data display a profile geometry that is similar to that of the temperature profile data shown in figure 3.10.5b. The calculated water vapour concentration profile data is shown in figure 3.10.6.

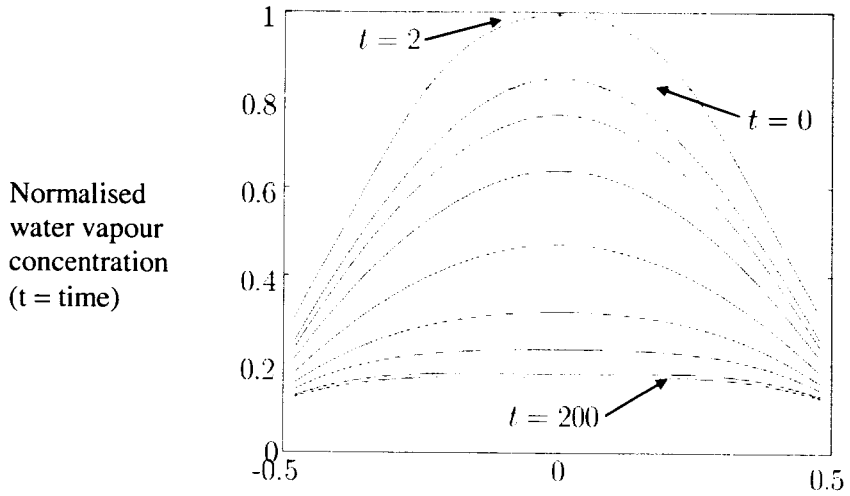

Figure 3.10.6: Calculated spatial profiles of scaled water vapour ($Y/Y_{max.}$).

While these current temperature and water vapour profile data display a parabolic profile form, this is not the case for the liquid phase. In the liquid phase case, the model predicts that the bagasse would adjust from an initially homogenous condition, to one where two concentration maxima exit near each side of the stockpile as shown in figure 3.10.7.

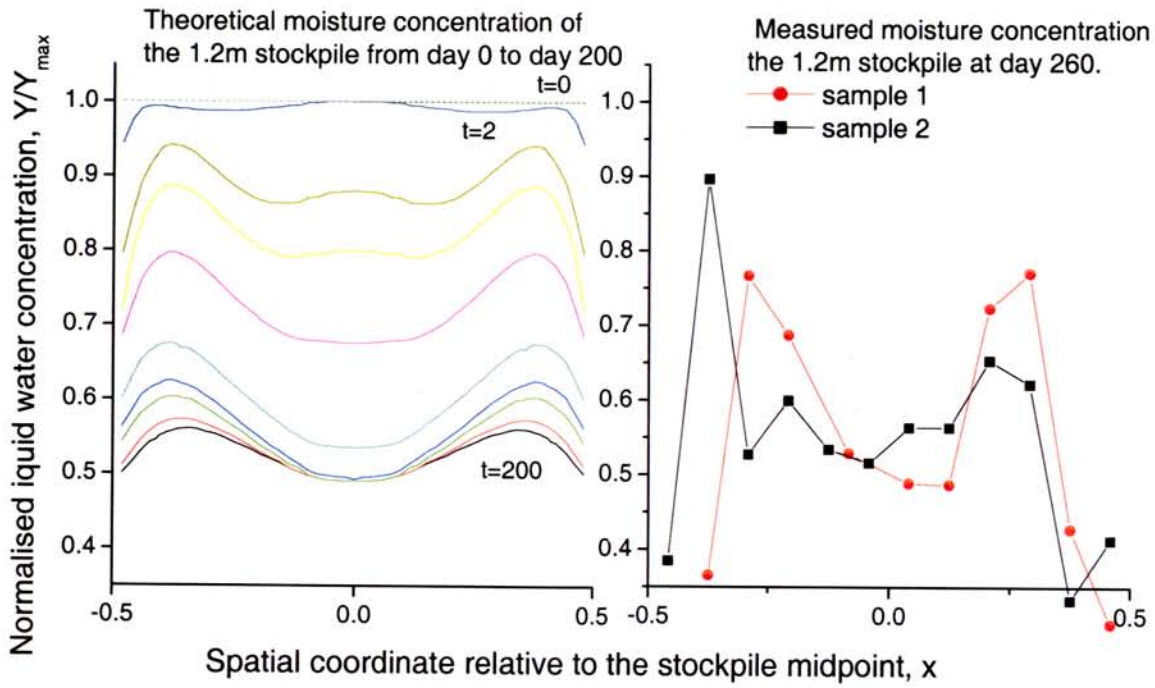

Figure 3.10.7: Spatial profiles of liquid water (X) for a 2.2m thick infinite slab of bagasse.

The liquid water distributions shown in figure 3.10.7 clearly indicate that the liquid water distribution has been influenced by the temperature distribution within the stockpile. The parabolic temperature distribution with a maxim centred about the stockpile midpoint, forces the liquid water phase outwards towards the cooler edges of the stockpile As such, a local minimum moisture value is found at the centre of the stockpile with the maximum moisture concentration occurring between the centre minimum and the stockpile surface. The above figure also includes the measured liquid water concentration data from the 1.2m wide stockpile at day 260. A comparison of these two sets of data reveal that the main features of the experimentally measured data have again been predicted.

The response of the stockpile to the ingress of liquid water has also been calculated. Figure 3.10.8 displays the calculated response of the stockpile after a percentage of the initial liquid water content is added at day 500

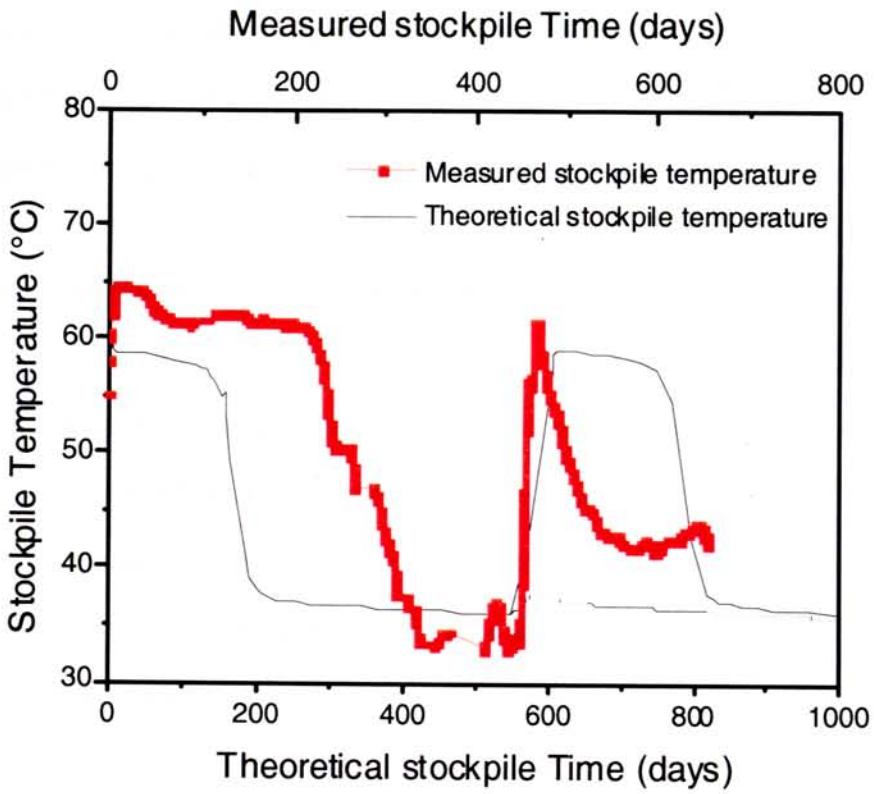

Figure 3.10.8: Calculated temperature history of a 2.2m stockpile which has been rewetted at day 500. (These data have been sourced from Sexton, 2001).

In the computer experiment shown in figure 3.10.8, the model calculations were initially allowed to develop for 570 days. During this time, the bagasse heated to a quasi-steady-state temperature of 57°C and then at approximately day 170, quickly cooled and approached a steady state temperature of approximately 36°C. After approximately 570 days of simulation, the liquid water content of the stockpile was uniformly increased, without perturbation of the stockpile temperature, to simulate the isothermal addition of liquid water. In the first computer experiment where 10% of the initial water content of the stockpile was added, a small temperature rise of a few degrees was calculated with this temperature gradually declining to the initial steady state value. This temperature rise is shown by the dotted temperature trace in figure 3.10.8. The model suggests that for small moisture perturbations, the temperature rise after the moisture addition is from the heat of wetting, rather than from the reinitiation of the wet oxidation reaction. For the case where the stockpile is subjected to a large moisture perturbation of a 70% addition of the initial moisture value, a significantly different temperature rise is calculated. In this second case, the system quickly returns to the quasi steady-state

temperature that existed prior to the extinction bifurcation event, a phenomenon that is essentially an extinction bifurcation reversal. Following the reinitiation of the wet oxidation reaction, the system again progressively expels water to the atmosphere until a second extinction bifurcation event occurs.

While model calculations required a stockpile with a thickness larger than that of the experimental 1.2m thick stockpile to produce comparative results, the model has nonetheless captured the main features of the 1.2m thick experimental stockpile remarkably well. Not only have the main experimentally observed temperature and moisture features been accounted for, but also the existence of a quasi steady state that has been shown to be dependent upon the bagasse moisture concentration. The extinction bifurcation event that occurs once the moisture concentration of quasi-steady-state stockpile reduces below a critical value has been demonstrated, as has the reignition of the wet oxidation chemistry following rewetting.

Macaskill, Sexton and Gray (1998) have completed computational simulations upon a stockpile of 1.5m width and 1.2m thick under the same environmental conditions as for the previously discussed theoretical results, but at an increased bagasse density. In the case of the 1.5m and 1.2 thick stockpile cases with a density of 125kg/m^3, the model predicts that heat will quickly escape from the stockpile due to its narrow width, and hence, cool to near ambient temperature. The maximum temperature and moisture concentration data for the 1.5m thick stockpile are shown in figure 3.10.9.

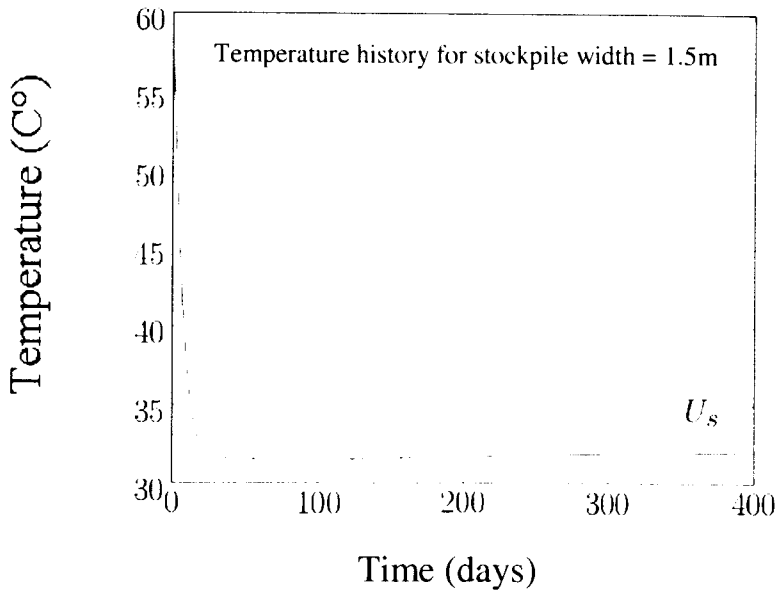

Figure 3.10.9a: Calculated temperature history for a 1.5m thick infinite slab of bagasse.

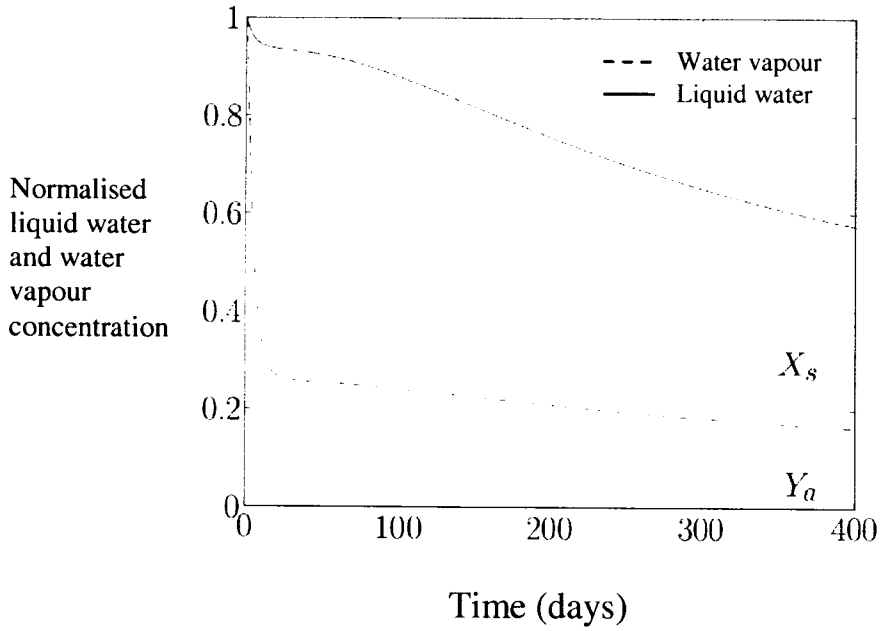

Figure 3.10.9b: Calculated moisture history for a 1.5m wide infinite slab of bagasse for a 400 day period.

In the above data the water vapour concentration is again responsive to the temperature of the stockpile. In this case, the water vapour concentration quickly reduces from an initially high value, to one close to the equilibrium concentration at ambient air temperature without achieving a quasi steady state. These current data also suggest, when they are compared to the computational data of the 2.2m wide stockpile, that the minimum width required to achieve the quasi-steady state lies between 2.1 and 1.5m. It should be further noted that while the experimental data of the 0.5m stockpile and this current computational data show qualitative similar trends, the consolidation problem is still present and its influence upon the experimental results needs be further investigated before a detailed comparison could be made.

Figure 3.10.10 shows the computational history of maximum temperatures within a stockpile of width 1.2m and densities of 125kg/m^3 and 500kg/m^3.

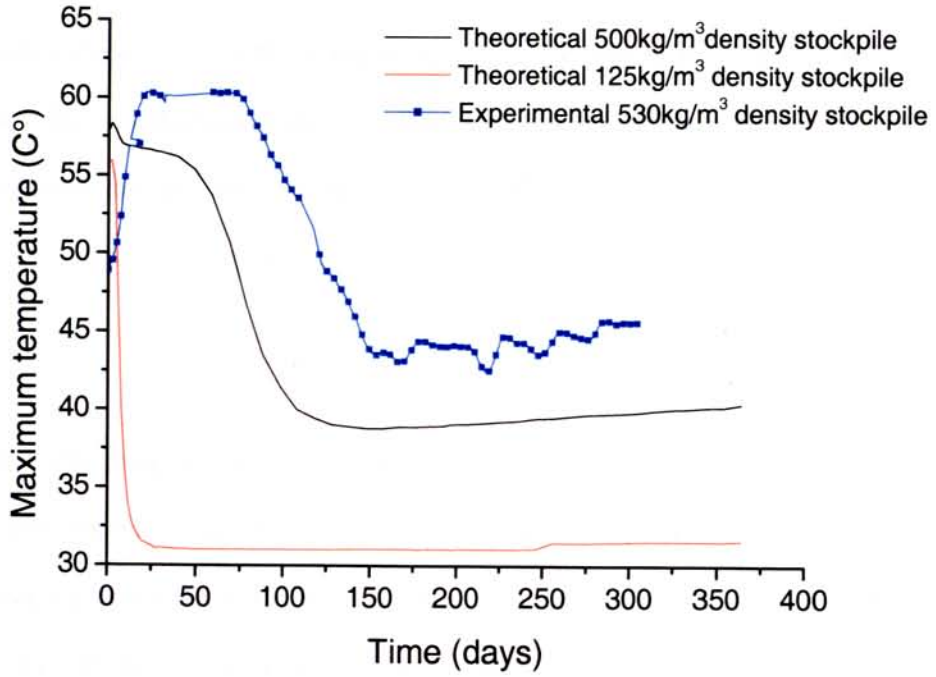

Figure 3.10.10: Calculated maximum temperature history for a 1.2m wide infinite slab of bagasse for densities of 125 kg/m^3 (red) and 500 kg/m^3 (black) and the corresponding experimental maximum temperature history for a stockpile simulating an infinite slab of bagasse at a density of 530 kg/m^3(blue).

When the two sets of theoretical data displayed in figure 3.10.10 are compared, it is clear that the higher density stockpile has heated to the quasi-steady-state temperature while the lower density stockpile has not. Notice also that these data suggest that at this increased density, the stockpile will remain at the quasi-steady-state temperature for a period of approximately 50 days. When this higher density calculated temperature data is compared to the corresponding experimental data, it can be seen that there is relatively good agreement with respect to both the quasi-steady-state temperature and the period that each stockpile remains at the quasi-steady state temperature. Notice that the slow increase in temperature of the experimental data after day 150 has also been accounted for by the model calculations. The calculated data suggest that this feature is a result of the stockpile drying to a moisture content that is less than that of the steady state value. The model suggests that this 'undershoot' is a response to a combination of the rate of drying at the higher density, combined with

the thermal time lag of the system with respect to temperature. Once the extinction bifurcation event occurs, the stockpile continues to expel moisture as it cools. Hence, the stockpile moisture concentration at the time when the stockpile approaches ambient temperature would be less than the equilibrium value at that temperature. An adjustment in moisture concentration follows, whereby the stockpile adsorbs atmospheric moisture to attain the equilibrium moisture concentration. The temperature rise is hence in response to the condensation of water vapour.

Clearly, these data suggest that the self-heating behaviour displayed by a stockpile is significantly dependent upon the bulk bagasse density. Given that the density was the least well-known parameter of the low-density experimental studies, it is conceivable that the bagasse density of the 1.2m stockpile was greater than 125kg/m^3, resulting in the lowering of the minimum width at which a quasi-steady-state can be achieved. Given this uncertainty in the bagasse density, the model shows a generally good correlation with the experimental results discussed in this chapter. Clearly, more work is required in this area before the detailed heating behaviour of bagasse stockpiles can be fully predicted from model calculations.

It should be noted that while the experimental studies of this chapter have concentrated on the self-heating of bagasse rather than the linkage between self-heating leading to thermal ignition. Macaskill, Sexton and Gray (1998) have theoretically examined conditions and geometries whereby self-heating bagasse stockpile are most likely to proceed to thermal ignition. The reader is referred to this publication for a detailed treatment of this aspect.

Both the experimental and computational data of this chapter have shown that it is possible to reduce bagasse stockpile moisture content from the initial moisture content of ~50% (wet basis) to a moisture content of between 15 to 25% (wet basis) using the heat generated by the wet oxidation chemistry. This aspect has potential for the sugar milling industry where bagasse is used as a fuel source since

bagasse with a reduced moisture concentration burns more efficiently and with less pollution than the corresponding higher moisture content sample. As a bonus, once the bagasse stockpile reaches its final steady-state condition, little self-heating occurs and the spontaneous combustion problem is significantly reduced or eliminated. This aspect clearly relies upon the availability of a low cost method to store the bagasse during the drying process, an aspect that may or may not be an industrially feasible option. Clearly, however, significantly more research would be required before this efficiency potential could be realised.

3.11. Conclusions

1. Bagasse stockpiles of sufficient width can quickly self-heat to a quasi-steady-state temperature following formation. While at this temperature, the stockpile loses moisture by evaporation and diffusion processes until the moisture concentration falls below a critical concentration, whereby the heat release rate drops significantly and the stockpile cools to a temperature close to ambient air temperature.

2. Following cooling from the quasi-steady-state temperature, the bagasse stockpile will remain stable with little heat being produced.

3. After cooling from the quasi-steady-state temperature, a stable bagasse stockpile may undergo further wet oxidation with an associated rapid thermal increase if the stockpile is sufficiently remoistened.

4. The Reaction-diffusion model of Stored Bagasse (Macaskill, Sexton and Gray, 1998) has captured the main self-heating features of the experimental results discussed in this chapter.

5. It is possible, using the energy generated by the wet oxidation reaction, to dry bagasse from its nominal moisture concentration of 50% (wet basis) to a minimum moisture concentration of between

15 and 25%. This aspect may have industrial applications if a cost effective storage method can be developed.

As an addition to the above conclusions, the use of insulation to simulate the self-heating behaviour of a much larger stockpile has proved useful for investigating the reliability of models describing self-heating behaviour.